CHEMPHYSCHEM

DOI: 10.1002/cphc.200700609

Chemistry of Energetically Activated Cumulenes—From Allene (H_2CCCH_2) to Hexapentaene ($H_2CCCCCCH_2$)

Xibin Gu,[a] Ralf I. Kaiser,*[a] and Alexander M. Mebel*[b]

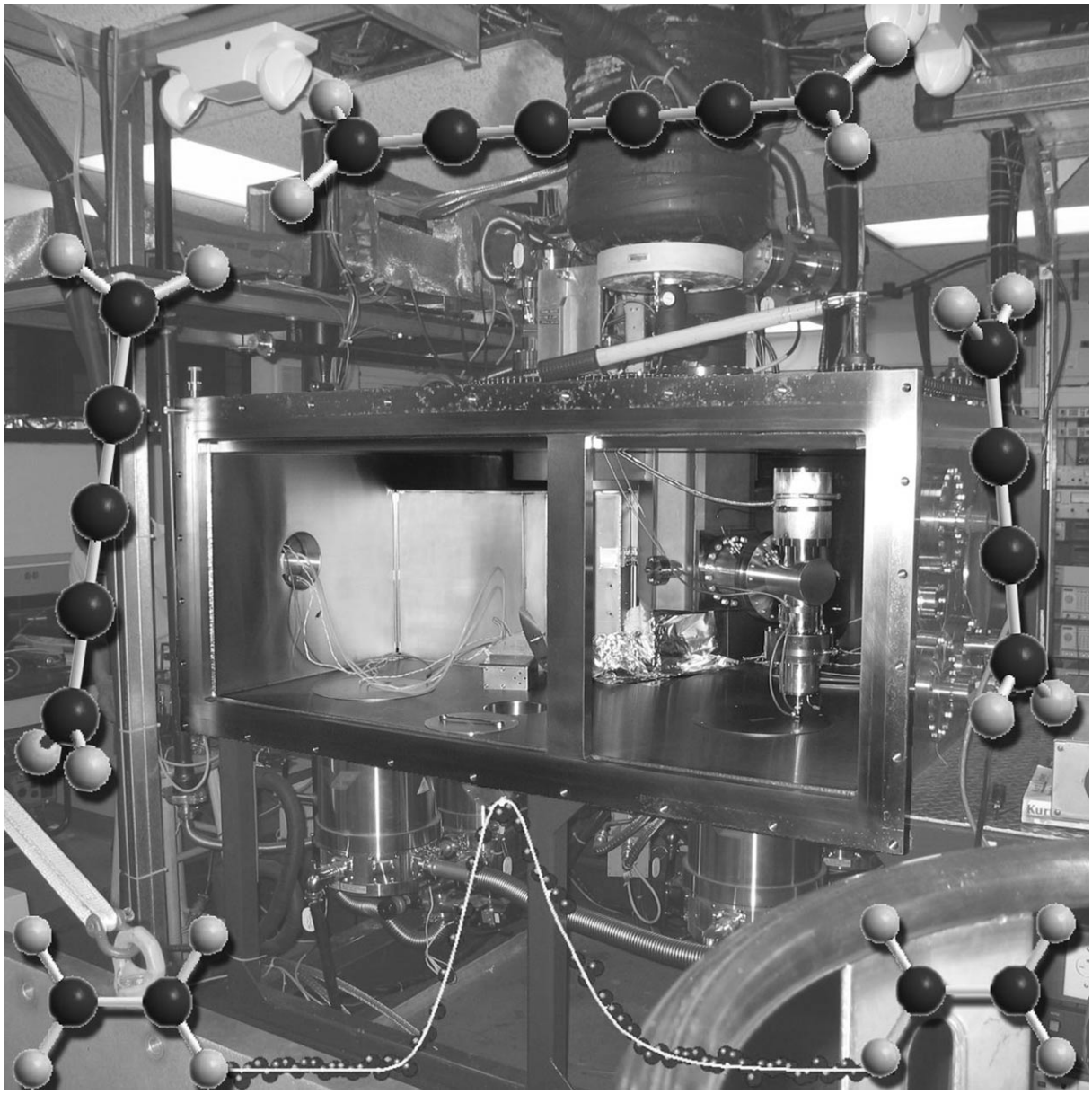

During the last decade, experimental and theoretical studies on the unimolecular decomposition of cumulenes ($H_2C_nH_2$) from propadiene (H_2CCCH_2) to hexapentaene ($H_2CCCCCCH_2$) have received considerable attention due to the importance of these carbon-bearing molecules in combustion flames, chemical vapor deposition processes, atmospheric chemistry, and the chemistry of the interstellar medium. Cumulenes and their substituted counterparts also have significant technical potential as elements for molecular machines (nanomechanics), molecular wires (nano-electronics), nonlinear optics, and molecular sensors. In this review, we present a systematic overview of the stability, formation, and unimolecular decomposition of chemically, photo-chemically, and thermally activated small to medium-sized cumulenes in extreme environments. By concentrating on reactions under gas phase thermal conditions (pyrolysis) and on molecular beam experiments conducted under single-collision conditions (crossed beam and photodissociation studies), a comprehensive picture on the unimolecular decomposition dynamics of cumulenes transpires.

1. Introduction

Cumulenes ($H_2C_nH_2$; $n \geq 2$) and the corresponding cumulene carbenes[1] (C_nH_2; $n \geq 2$) present important reaction intermediates in combustion flames,[2–4] chemical vapor deposition processes,[5,6] in the chemical evolution of hydrocarbon-rich atmospheres of planets and their moons such as Titan,[7,8] and in the chemistry of the interstellar medium such as in cold molecular clouds like TMC-1, circumstellar envelopes of the carbon star IRC+10216, and planetary nebulae like CRL 618.[9–16] Whereas lower members of the cumulene carbenes have C_{2v} symmetry and $^1A_1$ electronic ground states,[17–19] the situation for the closed-shell cumulenes is more complex.[20–22] Here, molecules having an even number of carbon atoms such as butatriene ($H_2C{=}C{=}C{=}CH_2$) and hexapentaene ($H_2C{=}C{=}C{=}C{=}C{=}CH_2$) belong to the D_{2h} point group (all four hydrogen atoms are in one symmetry plane);[23–26] on the other hand, cumulenes with an odd number of carbon atoms as found in propadiene/allene ($H_2C{=}C{=}CH_2$) and pentatetraene ($H_2C{=}C{=}C{=}C{=}CH_2$) dictate an inherent D_{2d} symmetry[27] and hence a pair-wise, staggered arrangement of the hydrogen atoms (Figure 1, Table 1). This correlates with the ^1A_g and $^1A_1$ electronic ground states for the even- and odd-numbered cumulenes, respectively.[28,29] The structures of these cumulenes also correlate with recent studies of ^{13}C nuclear magnetic resonance (NMR) paramagnetic shielding constants.[30] Considering the first excited triplet states of the cumulenes (Figure 1, Table 1), the situation is reversed. Here, even-numbered triplet cumulenes such as triplet butatriene ($H_2C{=}C{=}C{=}CH_2$) and hexapentaene ($H_2C{=}C{=}C{=}C{=}C{=}CH_2$) belong to the D_{2d} point group, whereas odd-numbered molecules like pentatetraene ($H_2C{=}C{=}C{=}C{=}CH_2$) have D_{2h} symmetry. Note that the C_{2v}-symmetric triplet allene presents an exception to this generalized principle.

Table 1. Compilation of the symmetry, ground electronic states, enthalpies of formation, singlet-triplet gaps, and the overall carbon-carbon lengths in cumulenes from propadiene to hexapentaene.

Cumulene	Symmetry/ electronic state	ΔH_f [kJ mol^{-1}] expt./theory	Singlet-Triplet gap[149] [kJ mol^{-1}]	C–C length[a] [Å]
H_2CCCH_2 propadiene	D_{2d}/X^1A_1	198.4 ± 12.5[146]/ 198.4[147]	215.6	2.604
H_2CCCCH_2 butatriene	D_{2h}/X^1A_g	(347.4)[148]/ 321.9[149]	173.7	3.894
$H_2CCCCCH_2$ pentatetraene	D_{2d}/X^1A_1	(481.4)[148]/ 465.1[22]	152.8	5.168
$H_2CCCCCCH_2$ hexapentaene	D_{2h}/X^1A_g	/586.0[149]	125.6	6.453

[a] From B3LYP/6-311G(d,p) calculations.

Due to their unique electronic structure,[31] cumulenes and their substituted counterparts have important technical potential as components of molecular machines.[32,33] Recent studies of these nanosystems also suggest that these molecules can be important building blocks in nano-electronics[34] and nanomechanics—a newly emerging field in structural chemistry.

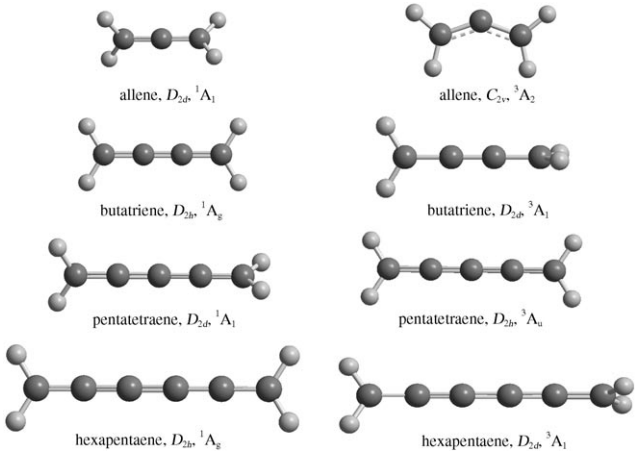

Figure 1. Structures of singlet (left) and triplet (right) cumulenes from allene to hexapentaene. The point groups and the symmetry of the electronic wave functions are also indicated.

[a] *Dr. X. Gu, Prof. R. I. Kaiser*
Department of Chemistry
University of Hawai'i at Manoa
Honolulu, HI 96822 (USA)
Fax: (+1) 808-9565908
E-mail: ralfk@hawaii.edu

[b] *Prof. A. M. Mebel*
Department of Chemistry and Biochemistry
Florida International University
Miami, FL 33199 (USA)
Fax: (+1) 305-3483772
E-mail: mebela@fiu.edu

Here, the terminal CH_2-group, for instance, can be rotated by 90° by the removal of two electrons from the highest occupied molecular orbital (HOMO).[35] The cationic forms also serve as models for molecular wires.[36–42] This makes cumulenic compounds relevant in the fields of molecular electronics,[43] nonlinear optics,[44] and molecular sensors[45] as well. For instance, cumulenic chains are stable under ultra-high vacuum conditions at temperatures lower than 250 K. They influence the electronic transport properties of the carbon-skeleton through a self-doping mechanism by pinning the Fermi level closer to one of the mobility gap edges. Upon heating above 250 K, the cumulenic species decay to form graphitic nanodomains embedded in an amorphous matrix.[46] It should be noted that cumulenes have significantly enhanced stability once they are coordinated to transition metals. This has been demonstrated, for instance, in the stabilization of butatriene[47] and hexapentaene[48] by iron-carbonyl complexes.

In combustion flames, cumulenes can lose hydrogen atoms via abstraction processes and unimolecular fragmentation of the cumulene molecules. This can lead to resonantly stabilized free radicals (RSFRs) in which the free electrons are delocalized over several carbon atoms. During the last decade, the investigation of the synthetic routes and chemical reactivity of these RSFRs have received particular attention due to their role in the formation of the first aromatic ring species[49–54] and of polycyclic aromatic hydrocarbons (PAHs) in combustion flames. These molecules are also believed to play a critical role in the formation of soot during the combustion of hydrocarbon fuels under oxygen-poor conditions.[55–57] In a RSFR, the unpaired electron is delocalized over at least two carbon atoms. This causes a number of resonant structures of similar importance.[58] Due to the delocalization, resonantly stabilized free hydrocarbon radicals are more stable than ordinary radicals, have lower enthalpies of formation, and normally form weaker bonds with stable molecules including molecular oxygen.[59–61] Such weakly bound addition complexes are not easily stabilized by collisions at high temperature. Therefore, RSFRs can reach high concentrations under combustion conditions making them important reaction intermediates to form complex, often polycyclic, aromatic hydrocarbons in flames.[62] These processes are both closely related to the growth of carbon clusters up to polycyclic aromatic hydrocarbons (PAHs) and carbon-rich interstellar grain particles in carbon-rich stars and to the synthesis of diamonds in hydrogen-poor preplanetary nebulae.[63]

Despite the importance of cumulenes in the chemical evolution of extreme environments (combustion flames, chemical vapor deposition [CVD], the interstellar medium) and promising technological applications such as molecular machines and as model systems for molecular wires, surprisingly little is known on the unimolecular decomposition and hence stability of these cumulenic structures. However, this information is crucial to model the chemical evolution of combustion flames and of distinct interstellar environments via chemical reaction networks reliably and to understand the role of cumulenes in the formation of complex, carbon-bearing molecules up to carbonaceous nano-particles (soot, interstellar grains). In this review, we present a systematic overview of the underlying unimolecular decomposition of cumulenes in extreme environments ranging from temperatures as low as 10 K (cold molecular clouds) up to a few 1,000 K (combustion flames). By focusing on reactions under thermal conditions (thermal chemistry via pyrolysis) and gas phase molecular beam experiments conducted under collision conditions (crossed beam and photodissociation studies), a comprehensive picture of the formation and unimolecular decomposition of cumulenes will emerge.

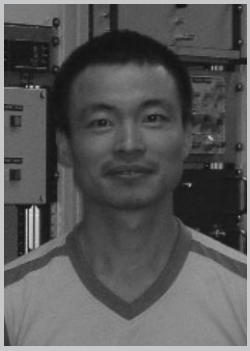

Xibin Gu obtained his Ph.D. in Chemistry from the Dalian Institute of Chemical Physics (China) in 2003. He joined the University of Hawaii at Manoa, Department of Chemistry, as a postdoctoral fellow in 2003 to conduct crossed molecular beam experiments on the dynamics and energetics of reactive intermediates relevant to the chemistry of combustion flames. In 2006, he was appointed Junior Researcher at The University of Hawaii.

Ralf I. Kaiser received his Ph.D. in Chemistry from the University of Münster (Germany) and Nuclear Research Center (Jülich) in 1994. He conducted postdoctoral work on the gas phase formation of combustion-relevant and astrophysically important molecules at UC Berkeley (Department of Chemistry). From 1997–2000 he received a fellowship from the German Research Council (DFG) to perform his Habilitation at the Department of Physics (University of Chemnitz, Germany) and Institute of Atomic and Molecular Sciences (Academia Sinica, Taiwan). After a brief stay at the Department of Chemistry, University of York (UK), he joined the Department of Chemistry at the University of Hawaii at Manoa in 2002 where he is currently a Professor of Chemistry.

Alexander M. Mebel studied chemistry at the Moscow Institute of Steel and Alloys and Kurnakov's Institute of General and Inorganic Chemistry of Russian Academy of Science in Moscow, Russia, where he received his Ph.D. in physical chemistry. Currently, he is Associate Professor at the Department of Chemistry and Biochemistry of Florida International University in Miami, Florida, USA. His current research interests involve theoretical quantum chemical studies of mechanisms, kinetics, and dynamics of elementary chemical reactions related to combustion, atmospheric, and interstellar chemistry.

2. Experimental Techniques

2.1 Thermal Chemistry

As probed in shock tubes, the breakdown of cumulenic structures can be initiated under *thermal conditions* via pyrolysis experiments at temperatures as high as 2000 K.[64–66] Here, a bath molecule or buffer gas molecule M can collide with the cumulene species $H_2C_nH_2$ and transfers energy to the rovibrational modes of the cumulene. This process yields an internally excited molecule $[H_2C_nH_2]^*$ [Eq. (1)]. The latter can lose its excess energy either by collision with another bath molecule M′ [Eq. (2)] or via fragmentation [Eq. (3)]. As these experiments are conducted under bulk conditions, wall effects can influence the outcome of the chemical reaction, and three-body reactions together with secondary reactions of the nascent reaction products can mask the outcome of a chemical reaction. This makes it difficult to identify the primary reaction products of pyrolytic studies unambiguously.

$$H_2C_nH_2 + M \rightarrow [H_2C_nH_2]^* \quad (1)$$

$$[H_2C_nH_2]^* + M' \rightarrow H_2C_nH_2 \quad (2)$$

$$[H_2C_nH_2]^* \rightarrow \text{products}. \quad (3)$$

2.2 Molecular Beams

Since the macroscopic alteration of interstellar environments and combustion flames consists of multiple elementary reactions that are a series of *bimolecular encounters* between atoms, radicals, and molecules, a detailed understanding of the decomposition of cumulenes occurring at the most fundamental, microscopic level is crucial. These are experiments under *single-collision conditions* in which particles of one supersonic beam are made to 'collide' only with particles of a second beam or are photolyzed by a laser beam. The crossed molecular beam technique represents the most versatile approach in the elucidation of the energetics and dynamics of elementary reactions, in particular of atom-radical and of radical-molecule reactions.[67–70] In contrast to bulk experiments, where reactants are mixed, the advantage of this approach is the capability to form the reactants in separate, supersonic beams. These features provide an unprecedented approach to observe the consequences of a single collision event, while preventing secondary collisions and wall effects. In principle, both reactant beams can be prepared in well-defined quantum states before they cross at a specific collision energy under single-collision conditions. The products can be identified via spectroscopic detection schemes such as laser-induced fluorescence (LIF)[71] or Rydberg tagging,[72] ion-imaging probes,[73–77] or via a quadrupole mass spectrometric detector (QMS). With QMS, the cumulenes can be formed in situ via chemical reactions and are chemically activated. For instance, reactions of carbon atoms (C)[78] and carbon clusters like dicarbon (C_2)[79] and tricarbon (C_3)[80] with ethylene (H_2CCH_2) and allene (H_2CCCH_2) can formally expand the carbon-skeleton by up to three carbon atoms yielding electronically and/or rovibrationally transient species [Eq. (4)]. In the gas phase, these intermediates have life times of a few picoseconds. Under single-collision conditions and hence the absence of stabilizing three-body collisions, these intermediates fragment via unimolecular decomposition [Eq. (5)].

$$H_2C_nH_2\ (n = 2,3) + C_m\ (m = 1-3) \rightarrow [H_2C_{n+m}H_2]^* \quad (4)$$

$$[H_2C_{n+m}H_2]^* \rightarrow \text{products} \quad (5)$$

Likewise, one supersonic beam can be replaced by a laser beam intersecting a molecular beam of the cumulene molecule. This leads us to the domain of the photochemistry of cumulenes [Eq. (6)] and the inherent photo-chemical activation and decomposition of cumulenes in their electronic ground and/or electronically excited states [Eq. (7)].

$$H_2C_nH_2 + h\nu \rightarrow [H_2C_nH_2]^* \quad (6)$$

$$[H_2C_nH_2]^* \rightarrow \text{products}. \quad (7)$$

By analyzing the fragmentation products under single-collision conditions, it is possible to monitor the primary reaction and photolysis products to gain unprecedented information on the stability, chemistry, and unimolecular decomposition of cumulenes. These studies are often pooled together with electronic structure calculations to provide a comprehensive picture on the chemical dynamics and underlying stability of singlet and triplet cumulenes.

3. Unimolecular Decomposition of Cumulenes

3.1 Propadiene

3.1.1 Thermal Decomposition

The thermal decomposition of propadiene/allene ($H_2C{=}C{=}CH_2$), the simplest and prototypical cumulene, was a subject of extensive experimental studies in the last five decades because of its relevance to soot formation in combustion processes. Collin and Lossing[81] investigated the fragmentation of allene and its structural isomer propyne (methylacetylene, CH_3CCH) back in 1957 using electron impact and derived upper estimates of their C–H bond dissociation energies of 340 and 347 kJ mol^{-1}, respectively. Later, several groups carried out more detailed investigations of allene pyrolysis.[64–66] In 1969, the product profiles from allene and propyne in a flow system in the temperature range of $T = 1173$–1430 K were measured and first-order rate constants for allene-propyne isomerization were determined by Levush et al.[66] They showed that under these conditions, the isomerization is faster than any decomposition process; however, the authors did not suggest detailed reaction mechanisms. This conclusion was confirmed by subsequent shock tube studies.[82–85] In their single-pulse shock tube measurements in the temperature range of 1040–1470 K, Lifshitz and co-workers observed both the decomposition and the isomerization processes. They suggested a chain mechanism initiated by a C–H bond cleavage both in allene and propyne. On the basis of the measured rate constants in the temperature range of 1300–2100 K, Kakumoto et al.[86] found the

activation energy for allene-propyne isomerization to be around 285 kJ mol^{-1}.Walsh and co-workers proposed that the allene-propyne isomerization takes place via the cyclopropene intermediate.[114–116]

Subsequently, Wu and Kern[87] studied high-temperature pyrolysis of allene in a shock tube at $T=1300$–2000 K and pressures of 0.2–0.5 atm; these authors derived, for the first time, a detailed reaction mechanism incorporating a primary dissociation process followed by numerous secondary reactions. The major pyrolysis products were shown to be acetylene (C_2H_2), diacetylene (C_4H_2), methane (CH_4), and benzene (C_6H_6), whereas traces of ethylene (C_2H_4), ethane (C_2H_6), vinylacetylene (C_4H_4), and triacetylene (C_6H_2) were also found. The mechanism describing the pyrolysis consists of 80 reactions, but the only primary reactions needed to describe the experimental results properly are the allene-propyne isomerization and the initial decomposition of allene and propyne to form the propargyl radical (C_3H_3) by hydrogen atom loss. Among secondary reactions, the most important are hydrogen atom additions to allene and propyne to produce C_3H_5 isomers such as the allyl radical, followed by their decomposition to various products and self-recombination of propargyl radicals (C_3H_3). This leads to the formation of benzene and eventually to the production of soot. Later, another study of the decomposition (and isomerization) by Hidaka and co-workers[88,89] confirmed the benzene formation and presented a quantitative mechanism similar to that of Wu and Kern.[87]

Most recently, Kiefer and co-workers[90] studied the unimolecular dissociation of allene and propyne using two complementary shock-tube techniques: laser schlieren (LS) and time-of-flight (TOF) mass spectrometry. The LS experiments were performed at 1800–2500 K and 70–650 torr, whereas the TOF results covered the temperature range of 1770–2081 K. The earlier conclusion that the dominant primary reaction path is a carbon-hydrogen bond rupture of either isomer did not change, although it was found that a small amount of molecular hydrogen (H_2) elimination may be possible from allene. Thermal rate constants for the hydrogen atom elimination from both allene and propyne were derived from the extrapolation of LS profiles to zero time using an extensive mechanism constructed to fit both the time profiles of LS gradients and the TOF product profiles. Since the LS technique can often eliminate the influences of secondary reactions, the carbon-hydrogen bond fission rates were accurately determined. They vary in the range of 2×10^9–2×10^{11} cm^3 mol^{-1} s^{-1} for $T=1800$–2500 K and are consistent with the carbon-hydrogen bond strength of 387 kJ mol^{-1} calculated for the methyl group in propyne by Bauschlicher and Langhoff.[91] The rate constants derived for the atomic hydrogen loss from allene and propyne differ only slightly, confirming that isomerization between the two structures is fast, but indicating that it is not so fast that separate rates cannot be resolved. Another important finding of Kiefer et al. is that the rate of the carbon-hydrogen bond fissions in propyne and allene measured in the high-temperature and low-pressure LS experiments cannot accurately be accounted for by Rice–Ramsperger–Kassel–Marcus (RRKM) theory unless the hindered rotation in propyne and allene is considered. As before, the authors detected acetylene, methane, diacetylene, and benzene as the major pyrolysis products. The formation of benzene (mostly via recombination of two propargyl radicals) is perhaps the most important matter in the allene/propyne pyrolysis, since it correlates with a high soot yield.[92]

Miller and Klippenstein[93] calculated the temperature- and pressure-dependent rate constants for the allene-propyne isomerization to be in the range between 10^4–10^{10} cm^3 mol^{-1} s^{-1} at temperatures in the range of 1200–2000 K, thus in quantitative agreement with the experimental values of both Hidaka et al.[88,89] and Wu and Kern.[87] The rate constant calculations for dissociation processes showed that the only significant products in this temperature range are C_3H_3 radicals plus atomic hydrogen; the total rate coefficient for the molecular hydrogen elimination is typically about three orders of magnitude (or more) smaller than that for carbon-hydrogen bond fission. Comparison of the theoretical predictions for the propyne and allene dissociation rate coefficients with the experimental results of Kiefer et al.[90] showed that the agreement between theory and experiment is very close; the calculations fall within the error bars of the measured data, with somewhat better agreement for allene. However, the computed dissociation rate constants for allene are about 10–20% faster than that of propyne, whereas the experiments show the opposite trend. According to Miller and Klippenstein it cannot be ascertained whether such small differences could be the fault of the theory or the experiment. For instance, a more accurate anharmonic state count in the theoretical treatment could reverse the calculated trend. Nevertheless, due to the excellent agreement between the calculated and experimental rate constants both for isomerization and dissociation reactions, one can conclude that the surface obtained by Miller and Klippenstein adequately describes the ground state of the C_3H_4 system. The major findings of the unimolecular decomposition of thermalized C_3H_4 molecules are compiled in Figure 2.

3.1.2 Molecular Beam Experiments—Photolysis

3.1.2.1 Flash Photolysis

The first ultra-violet (UV) flash photolysis experiments for allene and propyne were reported by Ramsay and Thistlethwaite in 1966,[94] who detected the same product, the propargyl radical, in both reactions. Two successive isotopic studies,[95,96] suggested that photolysis of propyne at 193 nm exclusively breaks the acetylenic carbon-hydrogen bond. Both observations can be reconciled if any CH_3CC produced in the flash photolysis experiment rearranges to form the lower energy propargyl isomer on the time scale of the experiment (25 μs). Further experimental studies of these processes have been carried out by using laser photolysis at various fixed wavelengths between 213 and 121.6 nm; the main focus of this work was the characterization of the primary fragments formed via molecular and atomic hydrogen loss pathways, the understanding of their competing formation processes, and the role of the allene-propyne isomerization.

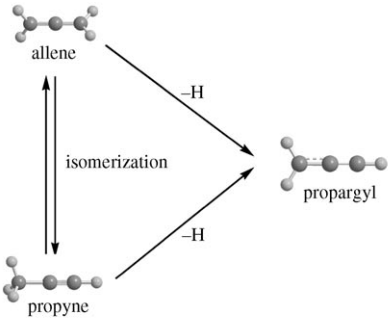

Secondary reactions:	Observed secondary products:	
$C_3H_3 + C_3H_3 \rightarrow C_6H_6$ (linear or benzene)	Major:	Minor:
C_3H_4 (allene/propyne) + H→ $C_2H_2 + CH_3 / C_3H_3 + H_2$	acetylene C_2H_2	ethylene C_2H_4
C_3H_4 (allene/propyne) + C$_2$H→ $C_3H_3 + C_2H_2$	diacetylene C_4H_2	ethane C_2H_6
C_3H_4 (allene/propyne) + CH_3→ $C_3H_3 + CH_4$	methane CH_4	vinylacetylene C_4H_4
$C_3H_3 + CH_3 \rightarrow C_2H_6 + C_2H / C_4H_6$	benzene C_6H_6	triacetylene C_6H_2
$CH_3 + CH_3 \rightarrow C_2H_6$		

Figure 2. Compilation of the principal reaction mechanisms in the thermal decomposition of allene.

3.1.2.2 Molecular Beam Studies—Time-of-Flight Spectroscopy

The first molecular beam study of the photodissociation of allene was performed by Jackson et al. in 1991.[97] Based on the translational energy distributions, the authors concluded that the decomposition takes place from allene molecules in their vibrationally excited electronic ground state. This result indicates that UV photochemistry of excited states of allene (as produced by absorption of 193 nm photons) indeed occurs via internal conversion to the vibrational continuum of the ground state. Thus, photoexcitation of allene can be used to generate vibrationally highly excited ("hot") molecules in the ground electronic state with their energy determined by the wavelength of the light. Photodissociation experiments can therefore be used to probe the unimolecular dissociation on the ground state potential energy surface (PES), similar to thermal decomposition or pyrolysis, but with well-defined internal energy and under collisionless conditions in molecular beams, i.e., at the zero-pressure limit. Jackson et al. measured time of flight (TOF) of the fragments of allene photolyzed at 193 nm and identified two primary dissociation channels, $C_3H_3 + H$ and $C_3H_2 + H_2$, with quantum yields of 0.89 and 0.11, respectively. The form of the translational energy distribution curve for the predominant hydrogen atom loss channel suggests the production of the propargyl radical; the distribution peaks at low translational energies and then monotonically decreases to the thermodynamic limit. This is indicative of a reaction occurring without a distinct exit barrier via a loose transition state. The primary products, propargyl and hitherto undefined C_3H_2 isomers were vibrationally excited upon formation and absorbed another photon to decompose to a variety of secondary products, such as $C_3H_3 \rightarrow C_3H_2 + H$, $C_3H + H_2$, and $C_2H_2 + CH$, or $C_3H_2 \rightarrow C_3 + H_2$, $C_2H + CH$, and $C_2H_2 + C$. Among the secondary product channels, the hydrogen atom loss from propargyl was found to be dominant (94%) followed by $C_3H + H_2$ (4%); however, the nature of the C_3H could not be unraveled. The remaining channels were minor routes. The production of the propargyl radical by the UV photolysis of allene is so efficient that it can be even used to measure high-resolution vibrational/rotational spectra of the propargyl radical.[98]

3.1.2.3 Molecular Beam Studies—Laser-Induced Fluorescence

In 1994, Jackson and co-workers revisited this system and measured the quantum state distribution of the secondary decomposition product tricarbon (C_3) from the "deep" multiphoton dissociation of both allene and propyne at 193 nm in a pulsed molecular beam.[99] Prior to this experiment, Lesiecki et al.[100] demonstrated that infrared (IR) multiphoton photolysis (with a carbon dioxide laser at 9.55 μm exciting the ν_9 CH_2 rocking vibration) of allene provides a source of tricarbon, which was detected by laser-induced fluorescence (LIF). Jackson and co-workers also utilized the LIF spectroscopy to measure C_3's rotational distributions in the 000 and 010 vibrational states. The distributions appeared to be cold and identical for C_3 derived from either allene and propyne. The results were explained by suggesting the following reaction mechanism: the initial photoexcitation of allene and propyne puts them in different Franck-Condon regions on their respective excited states. Direct dissociation from the different Franck-Condon regions would lead to distinct C_3H_2 product isomers with different internal energies, which in turn should give tricarbon products with different internal energies, contrary to the observations. For the rotational distributions of the observed tricarbon to be identical, one is forced to postulate that the photolyzed C_3H_2 intermediate should be the same for allene and propyne. One way to achieve this is by the conversion of electronically excited allene and propyne to the vibrationally excited C_3H_4 on the ground state PES before dissociation occurs. Once it is on this surface, a C_3H_4 molecule with internal energy of 620 kJmol^{-1} is above all barriers to isomerization, and the same intermediate is formed before dissociation. This agrees with the results of the allene and propyne pyrolysis experiments showing that the allene-propyne isomerization is faster than their decomposition. Alternatively, the equilibration may happen after the molecular hydrogen detachment from allene or propyne if the primary C_3H_2 product has enough internal energy for isomerization. The last possibility is that the photoexcited C_3H_2 isomer also undergoes internal conversion to the vibrationally hot ground electronic state and its isomerization on the ground state PES is faster than the molecular hydrogen loss. Any of these three scenarios can account for the observed identical rotational distributions of tricarbon from allene and propyne.

3.1.2.4 Molecular Beam Studies—Photoionization

Further photodissociation experiments, however, cast doubt that the unimolecular decomposition dynamics of allene and

propyne are completely identical. Ni and co-workers (1999)[101] used vacuum ultraviolet (VUV) laser photoionization at 118 nm in combination with TOF mass spectrometry to determine the photofragments of laser photodissociation of allene and propyne at 193 nm in a molecular beam. They confirmed atomic hydrogen elimination as the primary dissociation process for both of these molecules by detecting $C_3H_3^+$ ions. In addition, they observed molecular hydrogen elimination and also the carbene (CH_2) + acetylene channel for allene. The latter was observed for the first time, which is not surprising, because it is a minor channel responsible for only 1% of the total products as extrapolated to zero laser power. The contribution of the molecular hydrogen elimination was evaluated as 7%, slightly lower than the 11% obtained by Jackson et al.[97] This channel was found to include a multiphoton component of less than 10% of the total $C_3H_2 + H_2$ yield due to absorption of more than a single photon. Only the C_3H_3 (H-loss) and C_3H_2 (H_2-loss) fragments were detected in the photodissociation of propyne, with most of C_3H_2 resulting from a two-photon process. Ni et al. concluded that the different ratios of the various dissociation channels in allene and propyne points to a difference in dissociation mechanisms of these two molecules. The geometry on the excited state surface can influence the relative rates of internal conversion and direct dissociation, and the isomerization between allene and propyne might not be as fast as the dissociation. They also inferred that hydrogen atom production in propyne is likely to occur in the excited state, but in allene it takes place on the ground state surface.

Chang et al. followed up this study by measuring the ionic and luminous photofragments of allene excited with a focused laser beam at 193 nm,[102] such that the decomposition and ionization was caused by absorption of several UV photons. They performed laser-power dependence measurements to reveal the mechanisms accounting for the competition between dissociation and ionization in the excited states of allene and its photofragments. The major products observed were neutral carbon species (C, C_2), carbon ions (C_3^+, C_2^+, C^+), and methylidyne (CH). The yields of the hydrocarbon ions of $C_3H_n^+$ ($n = 1$–4) were relatively low compared with the yields of the abundant carbon ions. All the observed products were generated by multiphoton processes. A kinetic model was suggested to interpret the laser-power dependence of each photofragment and to illuminate the photodissociation/ionization mechanisms of allene. The model included the following processes ("→" and "⇒" denote one- or two-photon processes, respectively): production of C_3^+ (4 photons are required): $C_3H_4 \rightarrow C_3H_2 \rightarrow C_3 \Rightarrow C_3^+$; C_2^+ (5 photons): $C_3H_4 \rightarrow C_3H_2 \rightarrow C_3 \Rightarrow C_3^+ \rightarrow C_2^+$; C^+ (5 photons): $C_3H_4 \rightarrow C_3H_2 \rightarrow C_3 \Rightarrow C_3^+ \rightarrow C^+$; $CH(A^2D)$ (2 photons): $C_3H_4 \rightarrow C_3H_3 \rightarrow CH$; $C_2(d^3P_g)$ (4 photons): $C_3H_4 \rightarrow C_3H_2 \rightarrow C_3 \Rightarrow C_2(d)$; $C_2(D^1\Sigma_u^+)$ (3 photons): $C_3H_4 \rightarrow C_3H_2 \Rightarrow C_2$; and $C(^1P)$ (5 photons): $C_3H_4 \rightarrow C_3H_2 \rightarrow C_3 \Rightarrow C(^1D) \rightarrow C(^1P)$.Since the major ionic products detected are C_n^+ ($n = 1$–3), the authors concluded that the photodissociation of C_3H_n ($n = 1$–4) at 193 nm, with atomic/molecular hydrogen elimination or carbon-carbon bond rupture, is more favorable than the competing multiphoton ionization process in these hydrocarbons.

3.1.2.5 Molecular Beam Studies—Tunable Photoionization

In 1999, Neumark and coworkers[103] investigated the photodissociation dynamics of allene and propyne at 193 nm in molecular beams using two different techniques to photoionize the photofragments, namely electron impact ionization and tunable VUV light. Although they confirmed that the two major primary photodissociation product channels are $C_3H_3 + H$ and $C_3H_2 + H_2$, based on their measurements of photoionization efficiency (PIE) curves, they arrived to rather different conclusions than the previous groups, except for Satyapal and Bersohn,[95] and Seki and Okabe.[96] For instance, they assigned the C_3H_3 isomer formed from allene as propargyl, but that from propyne as propynyl (CH_3CC) and attributed the cleavage of the stronger acetylenic C–H bond in propyne instead of a weaker C–H-bond in the methyl group to the fact that the dissociation involves an electronically excited PES. The C_3H_2 fragments produced both from allene and propyne were assigned as vinylidenecarbene (H_2CCC), a small amount of which was also observed from secondary dissociation of C_3H_3. The $C_3H_3 + H$/$C_3H_2 + H_2$ branching ratios were evaluated as 64:36 and 56:44 for allene and propyne, respectively, which is at odds with the previous measurements by Jackson et al.[97] and Ni et al.[101] Four years later, DeSain and Taatjes[104] studied 193 nm photolysis of propyne using infrared laser absorption spectroscopy and reported even lower quantum yield of the C_3H_3 radical, 0.49 ± 0.1, though they disagreed on the identity of the C_3H_3 isomer produced, which, based on the observed infrared spectra, they concluded to be the propargyl radical. Interestingly, they also deduced that acetylene is a primary product of propyne photolysis, with a quantum yield of about 0.1.

3.1.2.6 Molecular Beam Studies—UV Spectroscopy

The question on the identity of the C_3H_3 isomer produced in photolysis of propyne lingered in the literature. In 2005, Fahr and Laufer[105] reported a study of UV absorption spectra of the radical transients produced in photodissociation of allene, propyne, and 2-butyne at 193 nm. In this work, the dissociation products were detected by time-resolved UV-absorption spectroscopy and through gas chromatographic/mass spectroscopic (GC/MS) analysis of the photolyzed samples. The spectral features measured for 193 nm photolysis of allene are in good agreement with the previously reported spectrum of the propargyl radical and thus the latter was concluded to be the dominant C_3H_3 isomer produced. The spectra obtained from 193 nm photolysis of $HCCCH_3$ (propyne) and CH_3CCCH_3 (2-butyne) are nearly identical but distinct from that for allene. This difference induced the authors to suggest that the observed absorption features for propyne and 2-butyne are likely to be composite with contributions from a number of transient species other than propargyl radicals. Based on the structural similarity of propyne and 2-butyne, Fahr and Laufer concluded that methyl (CH_3) and propynyl ($CH_3C \equiv C$) are likely to be among the photodissociation products of 2-butyne, whereas propynyl is likely to be the photodissociation product of propyne. They found some support for this conclusion in their GC/MS product analy-

sis of photolyzed 2-butyne samples, which showed the presence of C_2H_6 (formed by recombination of CH_3 radicals) and various C_6H_6 (including 1,5- and 2,4-hexdiynes) and C_4H_6 isomers likely formed in the $CH_3+C_3H_3$ reaction. However, a flaw in this consideration is the following: according to ab initio and RRKM calculations of product-branching ratios in the photodissociation of 2-butyne at 193 nm,[106] assuming both internal conversion to the ground state PES and statistical behavior, the C_3H_3 fragment is propargyl rather than propynyl. Isomerization of 2-butyne to 1,2-butadiene followed by the carbon-carbon bond cleavage in the latter to give propargyl plus methyl is faster than the direct dissociation of 2-butyne to propynyl and methyl. Therefore, it is likely that propargyl radicals are produced in the photodissociation of both propyne and 2-butyne. The difference in the UV absorption spectra of the radical transients could possibly be caused by a small contribution of propynyl formed on an excited state surface.

3.1.2.7 Molecular Beam Studies—Tunable Photoionization of Deuterated Molecules

In 2005, Neumark and coworkers[107] reinvestigated allene, propyne, and D3-propyne with photofragment translational spectroscopy (PTS) at 193 nm, also using tunable VUV synchrotron radiation or electron impact to ionize the fragments. They obtained TOF data and determined center-of-mass translational energy distributions ($P(E_T)$) and measured photoionization efficiency (PIE) curves. The $C_3H_3+H/C_3H_2+H_2$ branching ratio was found to be 90:10, regardless of precursor, in agreement with the results of Jackson et al.[97] and Ni et al.[101] The $P(E_T)$ distribution for each channel is also practically independent of precursor and both channels appear to occur following internal conversion to the electronic ground state, also in line with the conclusions of the previous studies. For allene, no evidence of the carbene (CH_2) + acetylene (C_2H_2) channel observed by Ni et al. was found; the authors attributed this to poorer kinematics in their experiment for the detection of fragments with relatively close masses. For the hydrogen atom loss, the $P(E_T)$ distribution is concentrated at very low translational energy, consistent with ground state dissociation to two open shell species C_3H_3+H without an exit barrier. The distribution for the minor $C_3H_2+H_2$ channel peaks well away from zero translational energy consistent with dissociation over an exit barrier. The shape of the PIE curve suggests that the vinylidenecarbene (H_2CCC) is the dominant product among C_3H_2 isomers in this minor channel. However, the authors did not rule out the formation of a small amount of the most stable C_3H_2 isomer, cyclopropenylidene, which would involve, as a precursor, cyclopropene, an intermediate along the allene-propyne isomerization pathway. Neumark and coworkers also concluded that the C_3H_3 species formed by hydrogen atom loss from propyne is dominantly the propargyl radical, although they have not completely excluded the possibility that there is some production of propynyl. As was the case for allene, the molecular hydrogen loss from propyne is relatively minor and the $P(E_T)$ distribution peaks well away from zero, consistent with ground state dissociation following internal conversion. The molecular hydrogen loss is disfavored by the tighter transition state associated with molecular elimination as opposed to bond scission, and the $P(E_T)$ distribution was consistent with dissociation over an exit barrier. The atomic versus molecular hydrogen loss branching ratios are largely identical for allene and propyne, even though the barrier heights for the two 1,1-elimination pathways are somewhat different by 33 kJ mol^{-1}. These results raise a question over how much isomerization occurs between propyne and allene prior to dissociation. This was addressed by interesting results obtained for D3-propyne. First, the authors looked at the D:H-branching ratio from photodissociation of CD_3CCH and found it to be approximately 1:1. Based on this, they deduced that the hydrogen atom loss from D3-propyne does not result from excited state dissociation to CD_3CC+H but is rather caused by isotopic scrambling prior to dissociation. This either takes place through isomerization to cyclopropene and back to propyne, giving CD_2HCCD, which could then lose a hydrogen atom to form D3-propargyl, or by isomerization to D3-allene, CD_2CCDH. The complete isotope scrambling would however be expected to result in a D:H-branching ratio of 3.3:1 rather than 1:1. To explain this discrepancy, the authors computed the densities of states for the possible reactions to form propargyl radical and H or D. It appeared that at the energies corresponding to 193 nm photoexcitation, the density of states for CD_2CCD+H is three times that of either $CHDCCD+D$ or CD_2CCH+D, thereby almost exactly compensating for the 3.3:1 D:H-ratio expected without considering product densities of states. Simply speaking, the hydrogen atom loss is more favorable thermodynamically (and kinetically) because the carbon-hydrogen stretching frequency is larger than that for carbon-deuterium and rupture of a carbon-hydrogen bond results in a larger reduction of the zero-point vibrational energy (ZPE) than in the case of carbon-deuterium bond. Therefore, isotopic scrambling of the hydrogen atoms in propyne competes effectively with the hydrogen atom loss. The question as to whether the hydrogen atom scrambling produces a significant allene population prior to dissociation was addressed by considering the molecular hydrogen loss channels, measuring HD:D_2-branching ratio, and PIE curves for C_3HD and C_3D_2 fragments. If no isomerization were to take place, then the molecular hydrogen elimination from D3-propyne would give only $D_2+DCCCH$ via a three-center transition state, because production of $HD+CCCD_2$ through a five-center transition state requires a much higher barrier. However, HD:D_2-branching ratios were measured to be between 1:1 and 1.5:1 and thus there should be significant isotopic scrambling in D3-propyne prior to a molecular hydrogen loss. The $P(E_T)$ and PIE curves help to identify the C_3HD and C_3D_2 fragments. The $P(E_T)$ distributions for HD versus D_2 are similar, whereas the PIE curves are identical within their error bars, indicating no difference between the C_3HD and C_3D_2 fragments. Moreover, these curves are more similar to the PIE curve for the molecular hydrogen loss from propyne than the corresponding curve for H_2 loss from allene. Based on this, the authors concluded that the HD- and D_2-loss channels are very similar, and there is a preference for forming C_3H_2 species with lower ionization potentials from propyne, that is, propargylene

(HCCCH) and cyclopropadienylidene, than from allene (vinylidenecarbene). This, however, only presents evidence that isotopic scrambling is not fast enough to fully eliminate the differences in photodissociation of allene and propyne.

3.1.2.8 Molecular Beam Studies—VUV Photodissociation

In 2000, Harich et al. studied the photodissociation dynamics of allene at a shorter wavelength with 157 nm VUV photons.[108] They confirmed the conclusion made by Ni et al.[101] that there exists three major decomposition channels, C_3H_3+H, $C_3H_2+H_2$, and $CH_2+C_2H_2$. According to the observed translational energy distributions, the dissociation was concluded rather to be statistical in nature and to occur on the ground electronic state PES after internal conversion. There is little or no reverse barrier for the hydrogen atom loss channel, but the translational energy distribution for the molecular hydrogen elimination peaks away from zero, at 75 kJ mol^{-1}, pointing to the existence of a significant reverse barrier for the production of $C_3H_2+H_2$, as is common for molecular hydrogen loss in hydrocarbons. The dynamics of the atomic and molecular hydrogen loss processes were found to be similar to those observed at 193 nm. A further insight was obtained for the $CH_2+C_2H_2$ products, namely a trace channel observed earlier by Ni et al. at 193 nm.[101] The translational energy distribution for CH_2 formation peaks at about 33 kJ mol^{-1}, indicating the existence of a small reverse barrier, and covering a broad energy range extending 25–293 kJ mol^{-1}. This means that at least a fraction of C_2H_2 products are acetylene molecules, although the vinylidene isomer (H_2CC) could be also produced. The latter can be formed via a carbon-carbon double bond cleavage in allene, but the formation of acetylene is expected to proceed via the cyclopropene intermediate. The H/H/CH_2-branching ratios were evaluated as 1:0.15:0.27 indicating that the increase of the photon energy and consequently the internal energy available to allene strongly favor the $CH_2+C_2H_2$ and $C_3H_2+H_2$ channels against the atomic hydrogen; recall that Ni et al. evaluated the branching ratios as 1:0.075:0.01 at 193 nm.[101]

Harich et al. also studied the photodissociation of propyne at 157 nm, including its deuterated counterparts CD_3CCH and CH_3CCD.[109] The hydrogen atom loss was observed both from the methyl group and from the ethynyl radical site. The hydrogen atom elimination from the methyl group was found to be a single dynamical channel and was concluded to be a statistical process occurring on the ground state PES after internal conversion. Alternatively, the hydrogen atom loss from the ethynyl (C_2H) group shows two distinguishable dynamic pathways with a ratio of 0.30 (fast) and 0.43 (slow), where the slow hydrogen atom products are attributed to statistical dissociation on the ground state surface and the fast products to dissociation in an excited electronic state. The overall branching ratio for the hydrogen atom elimination from the methyl and ethynyl group was evaluated to be 0.27:0.73. The yield of molecular hydrogen was much smaller than that of hydrogen atoms, with the molecular to atomic hydrogen branching ratio measured as 1:9.6. Comparison of the H_2, HD, and D_2 photoproducts from deuterated molecules indicated that the molecular hydrogen elimination process is not sensitive to the origin of the two hydrogen atoms and therefore scrambling of the hydrogen atoms is significant prior to dissociation at 157 nm. In addition, two different carbon-carbon bond breaking processes were also observed, producing CH_3+C_2H and $CH_2+C_2H_2$, with the relative branching ratio of 2.2:1, respectively. The existence of the latter channel also confirms that isomerization of propyne is significant prior to dissociation. Nevertheless, the observed differences in the photodissociation dynamics of allene and propyne at 157 nm clearly show that complete equilibration between the two isomers does not occur at these conditions.

3.1.2.9 Molecular Beam Studies—Rydberg Tagging

In 2002, Qadiri et al.[110] investigated the photodissociation dynamics of allene and propyne using the hydrogen atom Rydberg tagging method at 203.3, 209.0, and 213.3 nm. They found the translational energy spectra of the hydrogen atom formation channel to be practically identical for allene and propyne and to have the form well-reproduced by a statistical model. Qadiri et al. concluded the fragmentation to occur on the ground state surface and the isomerization between allene and propyne to precede the dissociation. In 2003, the same group[111] used the similar H(D) Rydberg tagging techniques to study the fragmentation dynamics of allene, propyne, and D3-propyne at 193 nm and arrived at the same conclusions based on the strong resemblance of the total kinetic energy release spectra of the H(D) atoms produced from H_2CCCH_2, H_3CCCH, and D_3CCCH. The authors contrasted their results to the earlier observations by Neumark and coworkers in their 1999 paper[103] and by Bersohn's group,[95] who inferred that the propynyl radical is formed in 193 nm photodissociation of propyne by a cleavage of the stronger acetylenic C–H bond. This likely occurs on an electronically excited state surface. Nevertheless, the later paper from Neumark's group in 2005[107] fundamentally agrees with the results of Qadiri et al. in that the H(D) loss processes from allene, propyne, and D3-propyne are preceded by isomerization and statistical equilibration. However, subtle differences were still observed for the other dissociation channels (H_2, D_2, and HD loss in the Neumark's study[107] and the observation of a trace $CH_2+C_2H_2$ channel from allene in the work of Ni et al.[101]), indicating that there is no full equilibration between allene and propyne before decomposition.

Qadiri et al.[111] extended their studies of the photofragmentation dynamics to the much shorter wavelength of 121.6 nm. In this case, they observed TOF spectra of the hydrogen and deuterium atoms, which were rather different for allene, propyne, and D3-propyne. They interpreted these differences by assuming two competing mechanisms for the H(D) loss from propyne. One involves selective cleavage of the acetylenic carbon-hydrogen bond on the excited electronic state surface where the photoexcitation energy is efficiently funneled to induce stretching of this bond. The second channel, with a slower distribution of H(D) atoms arises from internal conversion to a lower electronic state, isomerization and subsequent hydrogen atom loss. Interestingly, the data of the hydrogen

atom channel produced from 121.6 nm photolysis of allene are identical to those attributed to the second, statistical fragmentation channel of propyne. These results show that, as the wavelength shortens, the importance of the hydrogen atom loss channel involving the acetylenic hydrogen atom in propyne on the excited state PES increases.

3.1.2.10 Molecular Beam Studies—Inversion Mass Spectrometry

Hayakawa et al.[112] studied dissociation mechanism of electronically excited isomers of C_3H_4 using charge inversion mass spectrometry. In their experiment, neutral allene and propyne in excited states are formed by a neutralization reaction with alkali metal atoms (Cs and K), and then dissociated into neutral fragments, which are converted into negative ions and then detected by a mass spectrometer. Both $C_3H_3^-$ and $C_3H_2^-$ products are found for allene and propyne. The behavior of the branching ratio of molecular to atomic hydrogen loss indicats that dissociation in the higher excited state favors a molecular compared to atomic hydrogen loss. When two hydrogen atoms are eliminated, the dissociation occurs via molecular hydrogen rather than by two consecutive atomic hydrogen losses. Experiments with partially deuterated propyne (CD_3CCH) show that a HD elimination produces mainly vinylidene carbene D_2CCC or cyclopropenylidene isomers. However, the activation energy for the molecular loss channel should be higher than that for atomic loss pathway, although the heats of reaction for the former process are lower than those for the latter. The correlation between the product peak intensity ratios in the observed mass spectra shows that the weaker the carbon-hydrogen bond in allene or propyne, the more easily this bond cleaves. Finally, rupture of a carbon-carbon bond is found to be much less favorable than elimination of hydrogen atoms. The role of potential energy surfaces of excited electronic states is not well understood from this work, but it is likely that the electronically excited allene and propyne undergo fast internal conversion to the vibrationally excited ground electronic states prior to their dissociation.

3.1.2.11 Molecular Beam Studies—VUV Synchrotron Excitation

The most recent study of the photolysis of allene and propyne involves relaxation processes at much higher energies. Alnama et al.[113] used VUV synchrotron radiation in the excitation energy range of 7–30 eV (180–40 nm) and measured the visible fluorescence spectra of the excited neutral photofragments. Since only the electronically excited dissociation products are detected in this experiment, dissociation occurs on excited state surfaces and thus this report is complementary to the previous photolysis studies, in which mostly ground state fragments were measured (besides the work by Hayakawa et al.[112] and Chang et al.[102]). Note that at the photoexcitation wavelength of 157 nm (7.9 eV) and even 121.6 nm (10.2 eV) allene photodissociation was concluded to occur statistically, mostly on the ground state surface, whereas for propyne the role of excited state cleavage of the acetylenic C–H bond becomes significant at 157 nm. Alnama et al. were able to detect visible fluorescence from hydrogen atoms (4-2 and 3-2 Balmer lines), CH ($A^2\Delta$–$X\ ^2\Pi$) transition, and C_2 ($d^3\Pi_g$–$a^3\Pi_u$) "Swan's bands". The apparition thresholds of these excited products were determined and all processes leading to them were interpreted as fast and barrierless dissociation processes on the excited PESs. The authors concluded that at low energy of 7–16 eV, allene and propyne keep a "strong memory" of their initial structure and show differences in the observed spectra; though isomerization is already present, it is not dominant. Above 16 eV, increasingly fast isomerization as compared to neutral fragmentation is evidenced for both isomers. For example, around 17.5 eV, the sudden rise of the H_α emission signal in allene could be rationalized by an isomerization into propyne with the additional formation of the propynyl radical. Beyond 22 eV, the two isomers are no longer distinguishable either by their total fragment fluorescence or by their dispersed fragment fluorescence spectra. Thus, among the neutral relaxation processes occurring on the excited PESs and observed in this work, isomerization precedes neutral fragmentation in the high-energy range.

3.1.2.12 Electronic Structure Calculations

The experimental data described above can be better understood using ab initio calculations on the C_3H_4 potential energy surface. Yoshimine and co-workers first described detailed ab initio calculations of the ground state surface of C_3H_4.[114–116] They investigated the lowest energy pathways involving intermediate geometries and transition states and suggested the following sequence of reaction paths: allene (CH_2CCH_2)→1,2-H shift→vinylmethylene (CH_2CHCH)→ring closure→cyclopropene→1,2-H shift/ring opening→propenylidene(CH_3CHC)→1,2-H shift→propyne (CH_3CCH). These studies confirmed the proposal of Walsh and co-workers[117–119] that the allene-propyne isomerization takes place via the cyclopropene intermediate. The height of the isomerization barrier was found to be 275 kJ mol^{-1} above the zero-energy level of propyne, which itself lies 3 kJ mol^{-1} below allene. The barrier for the 1,3-H shift leading directly from allene to propyne was calculated to be much higher, at 397 kJ mol^{-1}. Further higher-level ab initio studies followed[120] and in the recent decade the allene-propyne isomerization was reexamined by Davis et al. at the G2-(B3LYP) level,[121] and the atomic and molecular hydrogen loss channels were computed by Mebel and co-workers at CCSD(T)/6-311 + G(3df,2p)//B3LYP/6-311G(d,p), along with calculations of the lowest excited states.[122,123] The most detailed account of the C_3H_4 PES in the ground state was given by Miller and Klippenstein in 2003,[93] who also utilized this surface to calculate microcanonical rate coefficients using RRKM theory, and to predict phenomenological rate constants for various reactions occurring employing several formulations of the master equation. Miller and Klippenstein confirmed the isomerization mechanism suggested by Yoshimine and co-workers (except that propenylidene does not appear to be a stable intermediate and vinylmethylene is only a metastable species)

and calculated the highest barrier on the reaction pathway to be 279 kJ mol^{-1} with respect to allene and to correspond to the initial 1,2-H migration step from allene to vinylmethylene. At 371 kJ mol^{-1}, the direct 1,3-H shift path from allene to propyne exhibits a much higher barrier. The energies for the atomic hydrogen loss processes to produce the propargyl radical were computed to be 373 kJ mol^{-1} and 376 kJ mol^{-1} for allene and propyne, respectively. The propynyl isomer (CH_3CC) lies 168 kJ mol^{-1} above propargyl[124] and so the hydrogen atom loss from the ethyl group in propyne requires 545 kJ mol^{-1}. The three-center molecular hydrogen elimination from allene yielding vinylidenecarbene (H_2CCC) goes via a barrier of 389 kJ mol^{-1}. The same product can be formed by five-center molecular hydrogen loss from propyne, but with a huge barrier of 532 kJ mol^{-1} relative to propyne. The 1,2-H_2 emission from the methyl group in propyne to form singlet propargylene (HCCCH) occurs via a lower barrier of 425 kJ mol^{-1}. Finally, the molecular hydrogen loss from cyclopropene producing the most stable C_3H_2 isomer (cyclopropadienylidene) requires a 350 kJ mol^{-1} barrier with respect to cyclopropene, but the latter itself resides 94 kJ mol^{-1} above allene. Note also that the endoergicities of the singlet $CH_2+C_2H_2$ and CH_3+C_2H product channels involving carbon-carbon bond cleavages computed at a similar G2M(MP2) level of theory are 454 kJ mol^{-1} and 513 kJ mol^{-1}, respectively.

Also, Jackson et al.[122] investigated surfaces for several excited electronic states of allene and deduced a scenario for internal conversion to the vibrationally excited electronic ground state. The most likely mechanism for the photodissociation of allene at 193 nm was suggested to involve as the initial step vertical excitation to the $^1B_1$ state. The difference between the energy of a photon and the adiabatic excitation energy for the corresponding equilibrium structure on the excited state PES is very large, about 327 kJ mol^{-1}. Therefore, the molecule formed in the excited electronic state should also be highly excited vibrationally. Particularly, since the allene molecule in the excited state tends to become planar, the normal mode corresponding to the internal CH_2 rotation should be excited. In the next stage, conversion into the vibrationally excited electronic ground state takes place by hopping from S_1 to S_0 on the seam of their crossing, which can happen at the planar C_{2v} symmetric geometries with a bent CCC group and would lead to vibrational excitation of the CC stretching and the CCC and CCH bending modes in the ground state. The existence of several crossing points between the excited and ground electronic states in the energy range below 628 kJ mol^{-1} indicates that internal conversion of allene to the ground state after photoexcitation should be fast, in line with the experimental observations in the allene photolysis.

For propyne photodissociation at 193 nm, Mebel et al.[123] suggested a mechanism that involves as the initial step vertical excitation to the ^1E state. Upon lowering the symmetry from C_{3v} to C_s, the first excited ^1E state splits into the $2^1A'$ and $^1A''$ components, both with *trans* and *cis* geometries. The geometry optimizations of these states give four distinct minima. The *trans* and *cis* forms of the $^1A''$ state have adiabatic excitation energies of 5.01 and 5.47 eV, respectively, and the geometry is characterized by the bent CCC and CCH groups in the molecule. The acetylenic CC bond is stretched from 1.20 to 1.36–1.39 Å, and the acetylenic carbon-hydrogen bond is elongated by 0.02–0.03 Å, whereas here only small changes in the geometry of the H_3C–C group is observed. Interestingly, the structures of the CCH group and the adiabatic excitation energies of the *trans*- and *cis*-bent $^1A''$ are close to those of the *trans*-^1A_u and *cis*-$^1A_2$ states of acetylene,[125] respectively. The differences between the photon energy and the adiabatic excitation energies of the S_1 ($^1A''$) and S_2 ($2^1A'$) equilibrium structures are 0.7–1.4 eV. The normal modes corresponding to the CCC and CCH bending and carbon-hydrogen stretching of the acetylenic hydrogen should be excited, while the methyl fragment is not affected. This sheds light on why the elimination of the acetylenic (but not methyl) hydrogen could be the major photodissociation channel occurring in the excited electronic state, although the acetylenic carbon-hydrogen bond is much stronger than the one in the methyl group. Also note that calculations by Cui et al.[126] show that the photodissociation mechanism of acetylene involves crossings between the S_1 and S_2 surfaces, as well as the S_2 and S_0 surfaces in the energy range of 6.1–6.3 eV along the pathway of the H atom elimination. As the excited-state surfaces for propyne and acetylene are similar, we speculated that the fast elimination of the acetylenic hydrogen in methylacetylene may occur by a similar mechanism: traveling along the S_1 and S_2 surfaces followed by the $S_2 \rightarrow S_0$ crossing and elimination of the H atom producing the propynyl radical (H_3CCC; $^2A_1$).[123] Thus, there exists a dynamical preference for hydrogen atom loss from the ethynyl group in propyne either on the excited state surface or immediately after internal conversion to the ground state. An alternative dissociation mechanism involves internal conversion into the ground state followed by redistribution of the energy between all vibrational degrees of freedom, in which case elimination of a methyl hydrogen on the vibrationally excited ground-state surface is statistically preferable. The major findings of the unimolecular photochemical isomerization and decomposition of C_3H_4 molecules are compiled in Figure 3.

3.1.3 Molecular Beam Experiments—Reactions

3.1.3.1 The C(^{3}P)/H_2CCH_2(X^1A_g) System

Crossed molecular beam experiments of ground and excited state carbon atoms with ethylene (H_2CCH_2) present a nice approach to access various intermediates on the C_3H_4 potential energy surface—among them singlet and triplet allene. The reaction of ground state carbon atoms was first investigated under single collision conditions at collision energies of 17.1 and 38.3 kJ mol^{-1} using the crossed molecular beams technique. This bimolecular reaction accesses the triplet allene structure. A detailed analysis of the product angular distributions and time-of-flight spectra of $m/z=39$ ($C_3H_3^+$) and $m/z=38$ ($C_3H_2^+$) suggests the existence of an atomic carbon versus atomic hydrogen replacement channel to form the propargyl radical (H_2CCCH) plus atomic hydrogen (Figure 4a).[127] Here, the carbon atom was found to add to the carbon-carbon

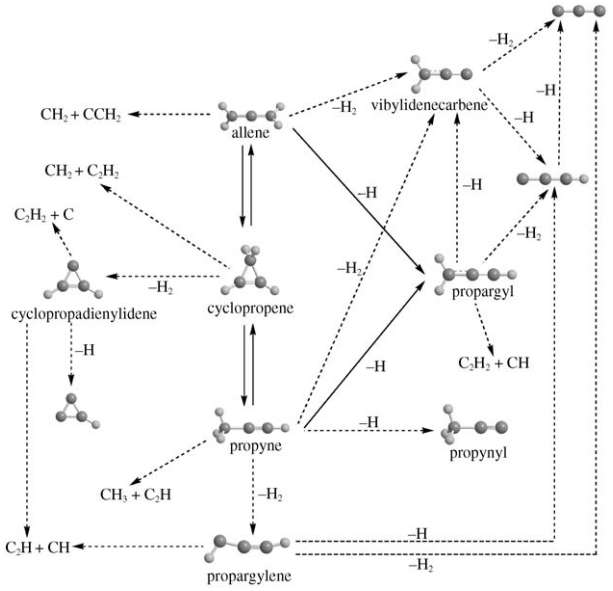

Figure 3. Compilation of the principal reaction mechanisms in the photochemistry of allene.

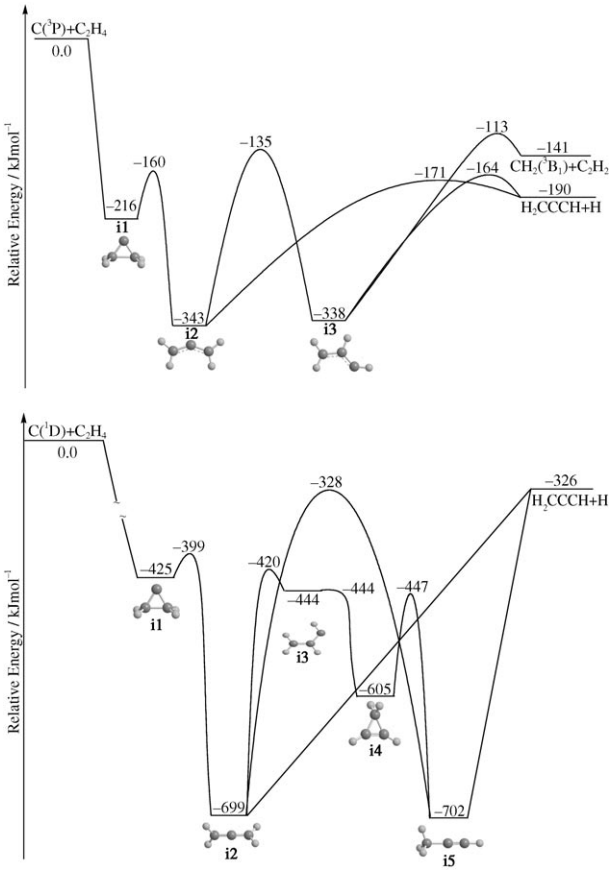

Figure 4. Relevant stationary points of the potential energy surfaces pertaining to the reactions of ground [$C(^3P)$, top] and excited state carbon atoms [$C(^1D)$, bottom] with ethylene (H_2CCH_2) and the involvement of singlet and triplet allene intermediates.

double bond without entrance barrier to form a triplet cyclopropylidene intermediate **i1.**[128–129, 130] The latter is stabilized by 216 kJ mol^{-1} relative to the reactants and isomerized via ring opening through a barrier of 56 kJ mol^{-1} to triplet allene **i2**. The triplet allene intermediate resides in a deep potential energy well of 343 kJ mol^{-1} and decomposes predominantly via a tight exit transition state located 19 kJ mol^{-1} above the separated products by atomic hydrogen loss to form the propargyl radical. Based on the energy dependence of the center-of-mass functions, the reaction with ethylene also shows also a second microchannel to form propargyl radicals via rather direct scattering dynamics; this contribution is quenched as the collision energy increased. Considering the energy dependence of the relative cross sections, the authors also predicted the existence of the $C_2H_2(X^1\Sigma_g^+) + CH_2(X^3B_1)$ channel. The finding correlates well with a theoretical study of this system. Here, Mebel and co-workers suggested that a minor fraction of about 7% of triplet allene **i2** rearranges via a hydrogen shift to vinylmethylene (**i3**) followed by fragmentation to atomic hydrogen plus the propargyl radical and to $C_2H_2(X^1\Sigma_g^+) + CH_2(X^3B_1)$ (2%).[128] All experiments and theoretical studies concur that an elimination of molecular hydrogen does not take place.

3.1.3.2 The $C(^1D)/H_2CCH_2(X^1A_g)$ System

Complementary to the triplet surface, the reaction of excited state carbon atoms [$C(^1D)$] with ethylene accesses the singlet C_3H_4 surface. This helps to unravel the unimolecular decomposition of chemically activated singlet allene under single collision conditions at collision energies of 48–104 kJ mol^{-1} (Figure 4b).[131] Similar to the triplet surface, the reaction is initiated via a barrierless addition of the carbon atom to the carbon-carbon double bond to form a singlet cyclopropylidene intermediate **i1**. The latter ring opens to singlet allene (**i2**). Due to the high collision energy, the lifetime of allene is very short; the inferred reaction dynamics are rather direct and dominated by a decomposition of singlet allene to form propargyl radicals plus atomic hydrogen. The short lifetime of the allene intermediate also hinders successive isomerization steps of singlet allene to three isomers: vinylmethylene (**i3**), cyclopropene (**i4**), and methylacetylene (**i5**).

3.2 Butatriene

3.2.1 Photochemistry

To date, neither shock-tube studies nor gas-phase photodissociation studies on the unimolecular decomposition of butatriene have been carried out. An in-depth literature search exposed only one matrix isolation study. Here, the photochemistry of butatriene is investigated by Wrobel et al.[132] using the matrix-isolation method in argon matrices at 10 K. The matrices were irradiated with 248 and 193 nm laser light and the products were identified by IR spectroscopy. The irradiation with 248 nm photons produced vinylacetylene ($H_2CCHCCH$), the van der Waals dimer of acetylene (HCCH…HCCH), and methylenecyclopropene ($H_2CC_3H_2$) as major products (Figure 5). Trace amounts of the allenylcarbene intermediate

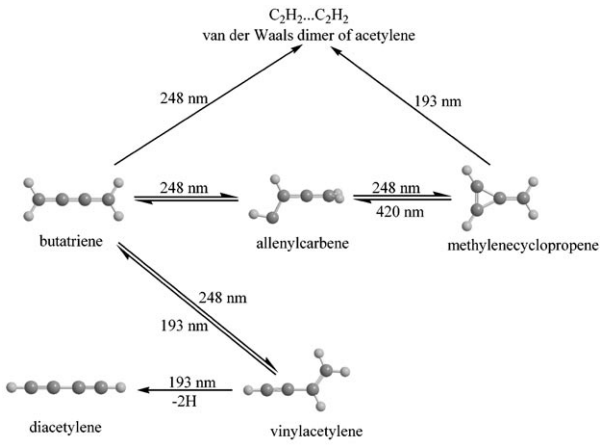

Figure 5. Compilation of reaction pathways in the photochemistry of butatriene under matrix conditions.

($H_2CCCHCH$) were also detected. The photochemical isomerization of butatriene to methylenecyclopropene appears to be reversible, as upon irradiation of the product mixtures with visible light with $\lambda > 420$ nm methylenecyclopropene rearranges back to butatriene. Irradiation at 193 nm results in a decrease of all absorptions of methylenecyclopropene and formation of butatriene. In addition, acetylene dimers are produced. The authors performed MP2 and DFT calculations and concluded that the butatriene-methylenecyclopropene rearrangement takes place predominantly on the singlet surface where the most plausible pathway is a two-(or multi-) step mechanism involving a 1,2-H migration followed by a vinylcarbene-cyclopropene rearrangement, which involves allenylcarbene as the key intermediate and requires a calculated barrier of 268 kJ mol^{-1}. Triplet allenylcarbene was also found to be a stable minimum on the surface. Similar photochemical matrix-isolation experiments on allenylcarbene reactivity by Aycard et al.[133] showed the formation of vinylacetylene and acetylene.

The observed isomerization and dissociation reactions of butatriene can be understood based on our G2M(RCC,MP2) calculations of the singlet C_4H_4 PES.[134] These calculations show that butatriene can rearrange to methylenecyclopropene by two different two-step pathways. The isomerization requires three-member ring closure and a 1,2-shift of one of the hydrogen atoms. These two processes can occur in different orders and hence two distinct rearrangement mechanisms were found. Along the first pathway, the first step is a hydrogen atom 1,2-migration leading to allenylcarbene. The calculated barrier for the hydrogen migration is 305 kJ mol^{-1}, and the resulting isomer $HCCHCCH_2$ lies 254 kJ mol^{-1} higher in energy than butatriene. $HCCHCCH_2$ is only a metastable intermediate, which easily undergoes ring closure to methylenecyclopropene overcoming a very small 2 kJ mol^{-1} barrier. Along the second possible pathway the ring closure occurs at the first step and is followed by the 1,2-H shift between two ring carbon atoms. The barrier for the ring closure is calculated to be 262 kJ mol^{-1} relative to butatriene and the cyclic intermediate formed after this rearrangement is only a metastable local minimum because the reverse ring-opening barrier is only about 1 kJ mol^{-1}. In the forward direction, the 1,2-H shift leads to methylenecyclopropene via a barrier of 63 kJ mol^{-1}. A comparison of the two mechanisms shows that the first pathway via allenylcarbene is energetically more favorable than the second because the highest barrier on the former (305 kJ mol^{-1} relative to butatriene) is 19 kJ mol^{-1} higher than that on the latter, 324 kJ mol^{-1}. In both cases, the 1,2-H shift is the rate-determining step. The most favorable isomerization channel of methylenecyclopropene leads to vinylacetylene. This process involves 1,2-H shift to the central carbon accompanied with a rupture of the carbon-carbon bond bridged by the migrating hydrogen atom with a barrier of 177 kJ mol^{-1}. Methylenecyclopropene can also dissociate into a number of different products. First, a cleavage of two single carbon-carbon bonds in the C_3 ring can result in the formation of acetylene plus vinylidene over a barrier of 260 kJ mol^{-1} and with an endoergicity of 244 kJ mol^{-1}. Vinylidene is a metastable intermediate, which rapidly isomerizes to acetylene, and apparently cannot be observed in the matrix isolation experiments. Alternative direct dissociation of methylenecyclopropene to two acetylene molecules exhibits a much higher barrier of 367 kJ mol^{-1}. The diacetylene (HCCCCH) plus molecular hydrogen products can be formed by 1,3-H_2 elimination overcoming a very high barrier of 432 kJ mol^{-1} relative to methylenecyclopropene (50 kJ mol^{-1} relative to butatriene). These products, which were observed by Wrobel et al., are more likely to be formed by a two-step mechanism from vinylacetylene including a hydrogen atom shift to form a terminal methyl group (methylpropargylene) followed by three-center molecular hydrogen elimination from this group, with a highest barrier of 384 kJ mol^{-1} relative to butatriene.

3.2.2 Molecular Beam Experiments—Reactions

The unimolecular decomposition processes of singlet and triplet butatriene molecules (H_2CCCCH_2) were investigated experimentally utilizing crossed molecular beams and theoretically via electronic structure calculations on the C_4H_4 PES. Here, we will first summarize the findings for the reactions of ground and excited state carbon atoms with allene (H_2CCCH_2) (Figure 6) and then compile the outcome of bimolecular collisions of singlet and triplet dicarbon molecules with ethylene (H_2CCH_2) (Figure 7). Formally, this expands the carbon skeletons of the allene and ethylene molecules by one and two carbon atoms respectively, to access the singlet and triplet structures of the butatriene.

3.2.2.1 The $C(^3P)/H_2CCCH_2(X^1A_1)$ System.

The crossed molecular beams technique was employed to investigate the reaction between ground state carbon atoms, C-(^3P_j), and allene, $H_2CCCH_2(X^1A_1)$, at two averaged collision energies of 19.6 and 38.8 kJ mol^{-1} (Figure 6 a).[135] Combined with electronic structure calculations,[135,136] it was suggested that the carbon atom can attack without entrance barrier at the central carbon atom or across the carbon-carbon double bond of allene yielding intermediates **i1** and **i2**, respectively. Since

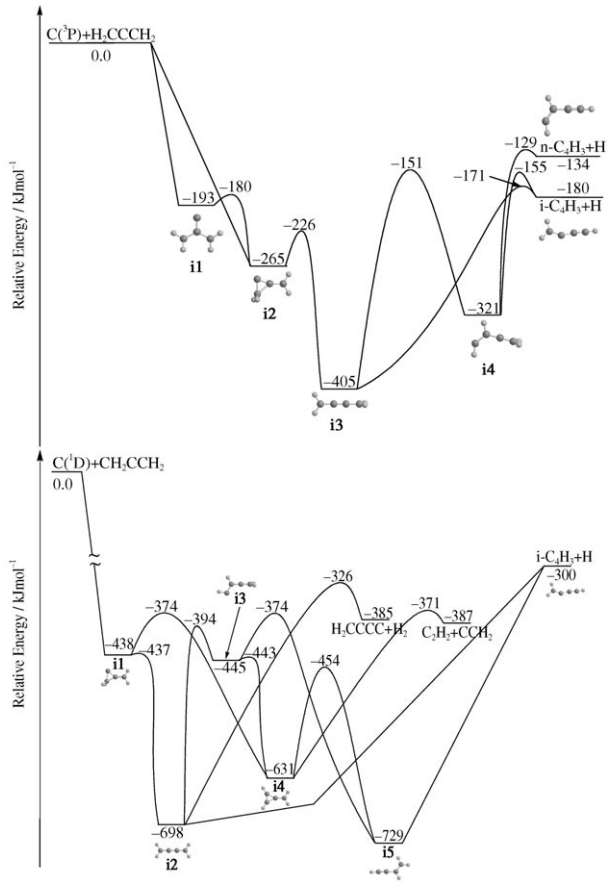

Figure 6. Relevant stationary points of the potential energy surfaces pertaining to the reactions of ground [$C(^3P)$, top] and excited state carbon atoms [$C(^1D)$, bottom] with allene (H_2CCCH_2) and the involvement of singlet and triplet butatriene intermediates.

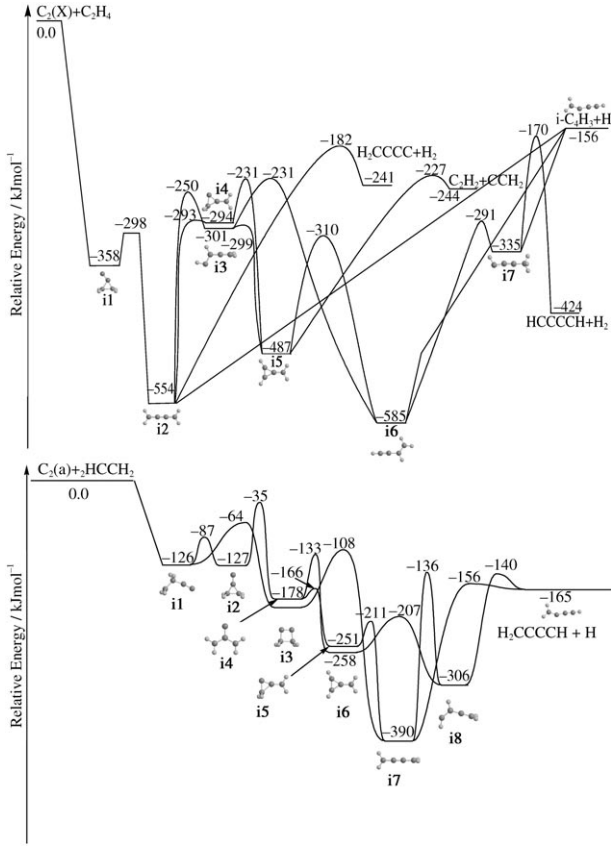

Figure 7. Relevant stationary points of the potential energy surfaces pertaining to the reactions of ground [$C_2(X)$, top] and excited state dicarbon molecules [$C_2(a)$, bottom] with ethylene (H_2CCH_2) and the involvement of singlet and triplet butatriene intermediates.

the reaction is dominated by large impact parameters, the formation of **i2** via an addition to one of the terminal carbon atoms seems to be the preferred reaction pathway. However, even if **i1** molecules are formed, they can isomerize to **i2** via a barrier located only 13 kJ mol^{-1} above **i1**. Intermediate **i2** then undergoes ring-opening to yield the triplet butatriene intermediate. Based on the center-of-mass translational energy distributions, the latter was found to have a life time in the order of 1 ps and decomposed via atomic hydrogen loss through a tight exit transition state to the i-C_4H_3 radical (1-butene-3-ynyl-2). These indirect reaction dynamics were also confirmed in electronic structure calculations. Here, statistical calculations predicted that the synthesis of the i-C_4H_3 radical presents the dominating decay channel of triplet butatriene; the energetically less stable *n*-C_4H_3 isomer was predicted to contribute to less than 1.5% to the signal. This structure, however, can be accessed only via intermediate **i4** which in turn can be formed by a hydrogen migration from triplet butatriene (**i3**).

3.2.2.2 The $C(^1D)/H_2CCCH_2(X^1A_1)$ System

The reaction of electronically excited carbon atoms with allene has been investigated only theoretically (Figure 6b).[134] Similar to the reaction of ground state carbon atoms, the dynamics were also found to be indirect and dictated by an addition of electronically excited carbon atoms to the carbon-carbon double bond of the allene molecule to yield intermediate **i1**. The latter can undergo ring-opening to form the singlet butatriene intermediate (**i2**). Singlet butatriene decomposes only via an atomic hydrogen product and a loose transituion state to the thermodynamically most stable *i*-C_4H_3 radical (1-butene-3-ynyl-2). Our calculations suggest that butatriene can also undergo two successive isomerization steps involving **i3** and **i4**. Here, both intermediates can undergo unimolecular fragmentation yielding acetylene and the vinylidene carbene isomer (CCH_2) products.

3.2.2.3 The $C_2(X^1\Sigma_g^+)/H_2CCH_2(X^1A_1)$ System

The unimolecular decomposition processes of singlet and triplet butatriene molecules (H_2CCCCH_2) were investigated in crossed molecular beams experiments of dicarbon molecules in the $X^1\Sigma_g^+$ electronic ground state and in the first excited $a^3\Pi_u$ state with ethylene at collision energies between 12.1 and 40.9 kJ mol^{-1}.[137,138] On the singlet surface, the dicarbon molecule is inferred to add without entrance barrier to the

carbon-carbon double bond forming a cyclic intermediate **i1** (Figure 7a). The latter undergoes ring-opening via a barrier of only 60 kJ mol^{-1} to the singlet butatriene intermediate (**i2**) which decomposes to the i-C_4H_3 isomer (1-butene-3-ynyl-2) plus atomic hydrogen via a loose exit transition state. However, the authors indicated that the sole existence of a singlet butatriene intermediate **i2** cannot account for the experimentally found asymmetry in the center-of-mass angular distributions at higher collision energies. Since singlet butatriene belongs to the D_{2h} point group, a C_2 axis is parallel to each principal rotational axis. This in turn classifies the butatriene intermediate as "symmetric"; each C_2 rotational axis can therefore interconvert the dissociating hydrogen atom giving this atom an equal probability to leave in the direction of either θ° or $\pi-\theta^\circ$. Consequently, the center-of-mass angular distribution would always be forward-backward symmetric at all collision energies—although the lifetime of the intermediate might be less than its rotation period. This has not been observed experimentally. Therefore, we have to conclude that there must be a second intermediate which decomposes to the *i*-C_4H_3 isomer via atomic hydrogen loss. Note that although the statistical calculations predict a molecular hydrogen pathway to be present at a level of about 14% relative to the atomic hydrogen pathway, there are various explanations as to why this channel was unobserved. First, dynamical (non-statistical) effects could favor the hydrogen atom loss compared to the molecular hydrogen elimination pathway. In this case, the RRKM calculations would effectively overestimate the importance of the molecular hydrogen channel. Alternatively, the authors could not determine the *relative* abundance of triplet versus singlet dicarbon in the beam; hence, even if the beam contains a 1:1 ratio of triplet versus singlet dicarbon, this would push the fraction of the molecular hydrogen level to about 7%—close to the sensitivity limit (about 5%) of the fits. The computations also predicted the existence of an acetylene (C_2H_2) plus vinylidene (CCH_2) channel on the singlet surface.[134]

3.2.2.4 The $C_2(a^3\Pi_u)/H_2CCH_2(X^1A_g)$ System

On the triplet surface (Figure 7b), triplet butatriene (**i7**) only holds a two-fold rotational parallel to the A principal axis. Therefore, only if triplet butatriene is excited to A-like rotations, the center-of-mass angular distribution will be forward-backward symmetric. Note that there are two additional C_2 axes at an angle of 45° intersecting the plane spanned by the *B* and *C* axes. However, it should be stressed that these axes are not parallel to any rotational axis, and can therefore not be considered. Therefore, triplet butatriene (**i7**) excited to *B*/*C* like rotations could account for the asymmetry of the center-of-mass angular distributions at higher collision energies. Considering the barriers involved in the isomerization of **i7** to **i8**, and comparing this number with the barrier of the atomic hydrogen loss from **i7** (about 9 kJ mol^{-1}), we expect that **i7** dissociates via hydrogen atom loss rather than undergoing isomerization to **i8**. Based on the triplet surface, the authors conclude that **i7** is the predominant decomposing intermediate on the triplet surface, which can account for the off-zero-peaking of the translational energy distributions and also for the asymmetry of the center-of-mass angular distributions at higher collision energies. Here, **i7** can be formed via the reaction sequence **i1**→**i3**→**i7** involving an initial addition of triplet dicarbon without an entrance barrier[139] followed by isomerization and ring opening.

3.3 Pentatetraene

3.3.1 Molecular Beam Experiments—Reactions

The experimental studies on the stability of singlet and triplet pentatetraene ($H_2CCCCCH_2$) are sparse and were conducted solely under single collision conditions in crossed beams experiments of singlet/triplet dicarbon with allene (H_2CCCH_2) and of singlet tricarbon with ethylene (H_2CCH_2). These investigations accessed both the singlet and triplet C_5H_4 potential energy surfaces. In this section, we first compile the findings for the reactions of ground and excited state dicarbon atoms with allene (Figure 8) and then summarize the conclusions of the bimolecular collisions of singlet tricarbon molecules with ethylene (Figure 9). Similar to the previous studies of atomic carbon dicarbon, and tricarbon with ethylene, the carbon-backbones of the allene and ethylene molecules are formally expanded by two and three carbon atoms respectively, to

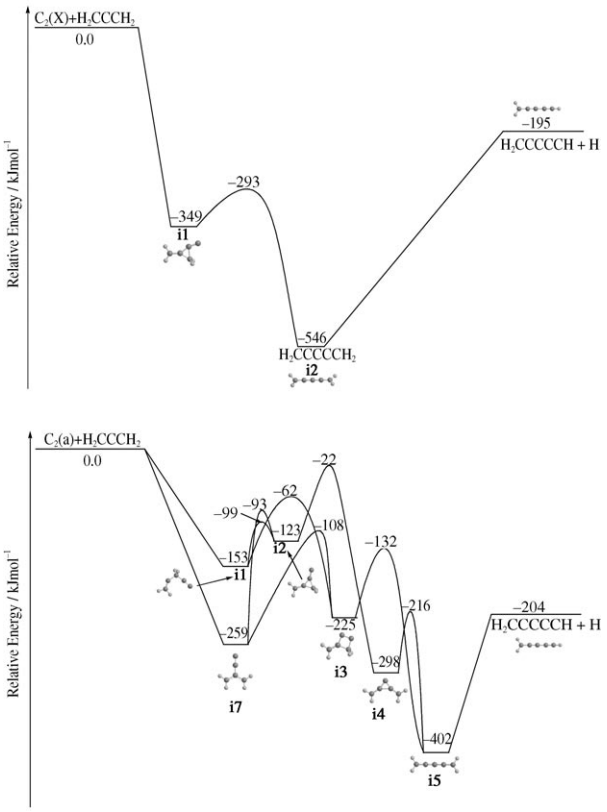

Figure 8. Relevant stationary points of the potential energy surfaces pertaining to the reactions of ground [C_2(X), top] and excited state dicarbon molecules [C_2(a), bottom] with allene (H_2CCCH_2) and the involvement of singlet and triplet pentatetraene intermediates.

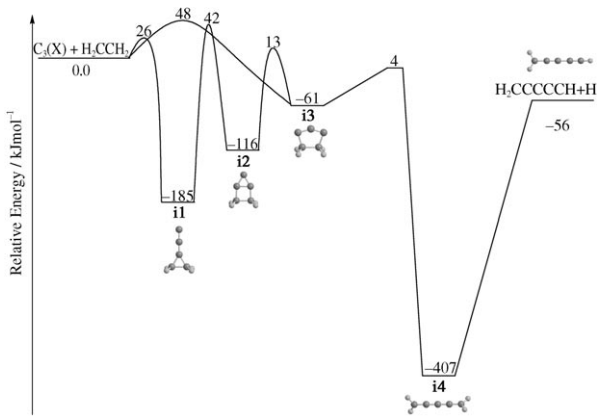

Figure 9. Relevant stationary points of the potential energy surfaces pertaining to the reactions of ground state tricarbon molecules ($C_3(X)$) with ethylene (H_2CCH_2) and the involvement of singlet pentatetraene intermediates.

form pentatetraene transient molecules on the singlet and triplet surfaces.

3.3.3.1 The $C_2(X^1\Sigma_g^+)/H_2CCCH_2(X^1A_1)$ System

The data suggested that the dicarbon molecule in its $X^1\Sigma_g^+$ electronic ground state added to the carbon-carbon double bond of the allene molecule forming a C_s symmetric **i1** collision complex without entrance barrier (Figure 8a).[137,140] The latter isomerized to pentatetraene **i2** which fragments without exit barrier via atomic hydrogen loss to the 2,4-pentadiynyl-1 radical [$C_5H_3(X^2B_1)$, $HCCCCCH_2$]. Detailed RRKM calculations[141] propose that a molecular hydrogen elimination pathway to form the $H_2CCCCC(X^1A_1)$ cumulene carbene via a tight transition state located 47 kJ mol^{-1} above the separated products does not compete with an atomic hydrogen loss pathway. Upper limits of 2–3% were derived; the calculated rate constant for the H loss from **i2** is a factor of 55.6–33.0 higher than the rate constant for the molecular hydrogen elimination from this intermediate. This verifies the experimental findings and the detection of only the atomic hydrogen loss channel.

3.3.3.2 The $C_2(a^3\Pi_u)/H_2CCCH_2(X^1A_1)$ System

On the triplet surface, the situation is more complex. Dicarbon can add to either the terminal or center carbon atom of the allenic carbon-carbon double bond to form **i1** and **i7**, respectively (Figure 8b). The rovibrationally excited collision complexes isomerize via **i3** to triplet pentatetraene (i**5**). The latter can decompose via a loose exit transition state through an atomic hydrogen loss, forming the 2,4-pentadiynyl-1 radical [$C_5H_3(X^2B_1)$, $HCCCCCH_2$]. The molecular hydrogen elimination channel was found not to compete. The authors also identified **i6** as the decomposing intermediate forming the 1,4-pentadiynyl-3 radical [$C_5H_3(X^2B_1)$, HCCCHCCH]. The involvement of **i6** can also be rationalized by inspecting the involved exit transition states.

3.3.3.3 The $C_3(X^1\Sigma_g^+)/H_2CCH_2(X^1A_g)$ System

The reaction of tricarbon with ethylene leads to the formation of the 2,4-pentadiynyl-1 radical ($HCCCCCH_2$) plus atomic hydrogen via a singlet pentatetraene intermediate.[142] To compare the experimental findings with the computed potential energy surface (Figure 9), the authors correlated the structure of the tricarbon and ethylene reactants with the reaction product and suggested feasible reaction intermediates. Here, the carbon backbone in the 2,4-pentadiynyl-1 radical is expanded by three carbon atoms compared to the ethylene reactant (H_2CCH_2). To connect the $HCCCCCH_2$ structure to the H_2CCH_2 reactant via C_5H_4 reaction intermediate(s), the reversed reaction of a hydrogen atom addition to the radical center at the CH group of the $HCCCCCH_2$ product forms the pentatetraene intermediate **i4** ($H_2CCCCCH_2$). To correlate the $H_2CCCCCH_2$ intermediates with tricarbon plus ethylene formally, it is necessary to expand the carbon-carbon backbone by three carbon atoms. In a similar way to the reaction of singlet dicarbon with ethylene, the experiments suggest that the tricarbon reactant eventually "inserts" into the carbon-carbon double bond of the ethylene molecule. Since it is not feasible for the tricarbon reactant to "insert" in a single step, tricarbon has to add to the carbon-carbon double bond of the ethylene reactant to form initially one or more cyclic C_5H_4 collision complex on the singlet surface. Based on the crossed beam studies, this process was found to have a characteristic threshold energy of 40–50 kJ mol^{-1}. The initial cyclic reaction intermediate(s) can isomerize to form eventually the pentatetraene intermediate ($H_2CCCCCH_2$). The computations confirm this postulated reaction mechanism (Figure 9).[143] Here, tricarbon can add in one step either side-on or end-on to the carbon-carbon double bond forming the intermediates **i3** and **i1**, respectively. Both addition processes have entrance barriers of about 26 and 48 kJ mol^{-1}. Intermediate **i1** can rearrange stepwise via **i2** to **i3**. Ultimately, **i3** undergoes ring-opening to form the postulated pentatetraene intermediate **i4** on the singlet surface. The pentatetraene molecule loses a hydrogen atom via a loose exit transition state, that is, a simple bond rupture process.

3.4 Hexapentaene

3.4.1 Molecular Beam Experiments—Reactions

3.4.1.1 The $C_3(X^1\Sigma_g^+)/H_2CCCH_2(X^1A_1)$ System

To date, only one experimental study exists on the unimolecular fragmentation of hexapentaene, namely, a crossed molecular beam study on the reaction of singlet tricarbon molecules with allene (H_2CCCH_2) (Figure 10). The experimental identification of the 1-hexene-3,5-diynyl-2 radical ($H_2CCCCCCH$) and the determination of an inherent threshold energy to the reaction in the order of 40–50 kJ mol^{-1} suggest that the tricarbon molecule adds to the π electronic system of the allene molecule followed by isomerization ultimately leading to cyclic reaction intermediates **i2** and **i3**. Both intermediates can be interconverted easily. The latter can also undergo a ring-opening process to form the hexapentaene molecule (**i4**) ($H_2CCCCCCH_2$), which

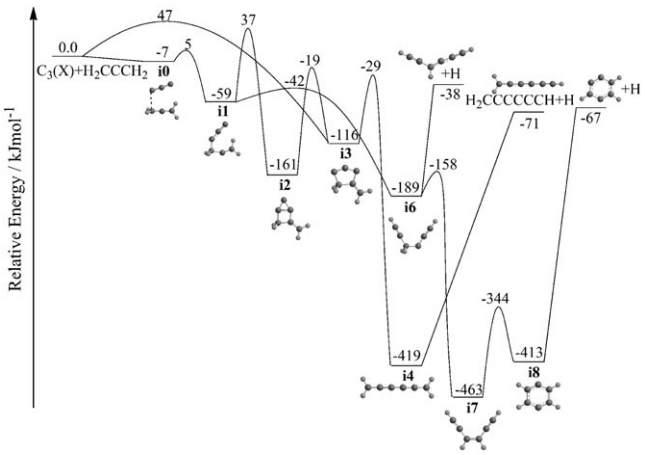

Figure 10. Relevant stationary points of the potential energy surfaces pertaining to the reactions of ground state tricarbon molecules ($C_3(X)$) with allene (H_2CCCH_2) and the involvement of singlet hexapentaene intermediates.

is stabilized by 419 kJ mol^{-1} with respect to the separated reactants. This reaction sequence of addition, isomerization, and ring-opening is similar to the one found in the tricarbon-ethylene system (3.3.3.3.). The short-lived hexapentaene molecule releases its excess energy via atomic hydrogen emission to form the 1-hexene-3,5-diynyl-2 radical product. Meanwhile, as seen in Figure 10, if the reaction behaved statistically, the formation of the other two products, cyclic C_6H_3 (4 kJ mol^{-1} less stable than 1-hexene-3,5-diynyl-2) and HCCCHCCCH (33 kJ mol^{-1} less stable than 1-hexene-3,5-diynyl-2) can also not be ruled out.

4. Summary and Outlook

In this review, we presented a systematic overview on the stability, formation, and the unimolecular decomposition of small to medium-sized cumulenes ranging from propadiene (H_2CCCH_2) to hexapentaene ($H_2CCCCCCH_2$) by focusing on reactions under thermal conditions (pyrolysis) and on molecular beam experiments conducted within the single collision regime (crossed beam and photodissociation studies). This succeeds excellent reviews of modern allene chemistry referring to classical synthetic approaches.[144] The pyrolysis studies of singlet propadiene (allene) suggest that the unimolecular dissociation dynamics are dictated by a simple carbon-hydrogen bond rupturing process leading to the propargyl radical (H_2CCCH) plus atomic hydrogen. This finding is similar to the unimolecular dissociation of chemically activated singlet and triplet allene intermediates. Here, the hydrogen atom emission and inherent synthesis of propargyl presents the dominating exit channel; to a small extent, carbon-carbon bond rupture also yields acetylene (C_2H_2) plus carbene (CH_2) on the triplet surface. As a matter of fact, all chemically activated cumulene structures from allene to hexapentaene, which are synthesized as reactive intermediates in the crossed beam reactions of carbon atoms, dicarbon, and tricarbon with ethylene (H_2CCH_2) and allene (H_2CCCH_2), lose their internal energy predominantly via atomic hydrogen emission and the formation of doublet radicals of the generic formula C_nH_3 (H_2C_nH; $n=3$–6) (Figure 11; Table 1 and Table 2). These open-shell species are resonantly stabilized free radicals which are of crucial importance as transient species in the underlying chemical processing of hydrocarbon flames and circumstellar envelopes of carbon stars to form polycyclic aromatic hydrocarbons. In the crossed beam studies, molecular hydrogen emission was not observed. In agreement with theory, the molecular hydrogen channel should be only of minor importance, typically in the order of 5%. Also, carbon-carbon bond ruptures of the singlet and triplet cumulenes are less important than the competing hydrogen atom loss pathways. It should be emphasized that the unimolecular decomposition of thermally and chemically activated cumulenes such as allene differs somewhat from the photochemically induced fragmentation. In the case of allene—the only cumulene studied in molecular beams—the atomic hydrogen emission and the inherent synthesis of the

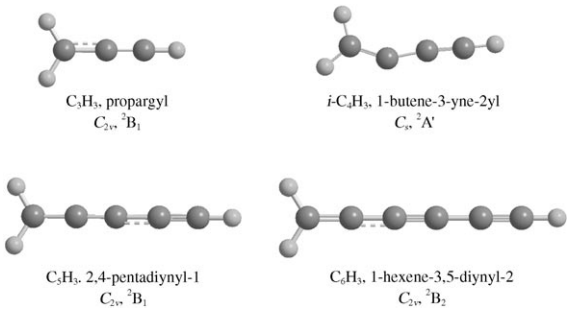

Figure 11. Structures of doublet radicals formed in the unimolecular decomposition of singlet and triplet carbenes. The point groups and the symmetry of the electronic wave functions are also indicated. Note that a C_{2v} symmetric i-C_4H_3 stationary point only presents a transition state.

Table 2. Compilation of the symmetry, ground electronic states, enthalpies of formation, and the overall carbon-carbon lengths for the doublet radicals formed in the unimolecular decomposition of the corresponding cumulenes.

Species	Symmetry/ electronic state	ΔH_f [kJ mol^{-1}] expt./theory	C–C length [Å]
C_3H_3 H_2CCCH propargyl	C_{2v}/X^2B_1	356.6[150]/355.0[147]	2.589
i-C_4H_3 H_2CCCCH 1-butene-3-ynyl-2	C_s/X^2A'	504 ± 10/498.1[151]	3.818
C_5H_3 $H_2CCCCCH$ 2,4-pentadiynyl-1	C_{2v}/X^2B_1	600 ± 10/571.4[152]	5.146
C_6H_3 $H_2CCCCCCH$ 1-hexene-3,5-di-ynyl-2	C_{2v}/X^2B_2	733 ± 10/734.2[149]	6.412

propargyl radical product remains the dominant channel (64–90%). Due to the enhanced energy content of photochemically activated cumulene, the molecular hydrogen loss pathway to form vinylidenecarbene (H_2CCC) becomes increasingly important as the photolysis wavelength is reduced (8–30%). Similarly to the thermal activation of the allene, carbon-carbon bond ruptures play only a minor role in the dynamics at a level of typically 1%.

The crossed molecular beam experiments also help us to extract generalized concepts on the formation and decomposition of cumulenes under single collision conditions. All reactants (ground-state and excited-state carbon atoms and dicarbon molecules, and ground state tricarbon) first add to the π electronic system of the ethylene and allene reactants. In strong contrast to the barrierless addition of atomic carbon and dicarbon, the reactions of tricarbon molecules display significant threshold energies in the order of 40–50 kJ mol^{-1}. These initial collision complexes can undergo successive isomerization ultimately leading to singlet/triplet cumulene species. De facto, the carbon, dicarbon, and tricarbon reactants "insert" into the carbon-carbon double bond of the ethylene and allene molecules in a multi-step reaction sequence. The cumulenes decompose predominantly via atomic hydrogen loss pathways to form resonantly stabilized free hydrocarbon radicals. This generalized reaction sequence as compiled in Equation (8) and the crossed beam reactions can be expanded in principle to more complex cumulenes like butatriene and carbon molecular reactants such as C_4 and C_5. This could extend the reaction dynamics studies to cumulenes as complex as heptahexaene ($H_2C_7H_2$), octaheptaene ($H_2C_8H_2$), and nonaoctaene ($H_2C_9H_2$) and their corresponding hydrogen-deficient doublet radicals H_2C_7H, H_2C_8H, and H_2C_9H—transient species which cannot be synthesized by classical organic synthesis. In a similar way as for linear and cyclic C_3H isomers[145]—both isomers were recently produced in situ via laser ablation of graphite and seeding the ablated carbon atoms in acetylene gas which also acted as a reactant—it should be feasible to produce the cumulenes $H_2C_nH_2$ and their H_2C_nH radicals in situ. This is of crucial importance to extract their thermodynamical properties such as ionization potentials by selectively photoionizing these species via tunable vacuum ultraviolet photons and recording the VUV wavelength dependent TOF spectra of the ionized molecules.

$$H_2C_nH_2\ (n = 2,3) + C_m\ (m = 1 - 3) \rightarrow [H_2C_{n+m}H_2]^* \rightarrow H_2C_{n+m}H + H \quad (8)$$

Acknowledgements

The work was supported by the US Department of Energy-Basic Energy Sciences [DE-FG02-03ER15411 (X.G., R.I.K.) and DE-FG02-04ER15570 (A.M.M.)].

Keywords: ab initio calculations · cumulenes · radicals · reaction mechanisms · reactive intermediates

[1] L. Brandsma, *Best Synthetic Methods: Acetylenes, Allenes and Cumulenes*, Elsevier, Amsterdam, **2003**.
[2] T. R. Melton, F. Inal, S. M. Senkan, *Combust. Flame* **2000**, *121*, 671–678.
[3] N. Hansen, S. J. Klippenstein, J. A. Miller, J. Wang, T. A. Cool, M. E. Law, P. R. Westmoreland, T. Kasper, K. Kohse-Hoeinghaus, *J. Phys. Chem. A* **2006**, *110*, 4376–4388.
[4] C. Huang, L. Wei, B. Yang, J. Wang, Y. Li, L. Sheng, Y. Zhang, F. Qi, *Energy Fuels* **2006**, *20*, 1505–1513.
[5] L. Ravagnan, F. Siviero, C. Lenardi, P. Piseri, E. Barborini, P. Milani, C. S. Casari, A. Li Bassi, C. E. Bottani, *Phys. Rev. Lett.* **2002**, *89*, 285506.
[6] C. Hallin, I. G. Ivanov, T. Egilsson, A. Henry, O. Kordina, E. Janzen, *J. Cryst. Growth* **1998**, *183*, 163–174.
[7] D. Cremer, E. Kraka, H. Joo, J. A. Stearns, T. S. Zwier, *Phys. Chem. Chem. Phys.* **2006**, *8*, 5304–5316.
[8] J. A. Stearns, T. S. Zwier, E. Kraka, D. Cremer, *Phys. Chem. Chem. Phys.* **2006**, *8*, 5317–5327.
[9] P. M. Woods, T. J. Millar, E. Herbst, A. A. Zijlstra, *Astron. Astrophys.* **2003**, *402*, 189–199.
[10] F. J. M. Rietmeijer, A. Rotundi, *Polyynes* **2006**, 339–370.
[11] J. A. Hodges, R. J. McMahon, K. W. Sattelmeyer, J. F. Stanton, *Astrophys. J.* **2000**, *544*, 838–842.
[12] S. J. Blanksby, J. H. Bowie, *Mass Spectrom. Rev.* **1999**, *18*, 131–151.
[13] A. J. Apponi, M. C. McCarthy, C. A. Gottlieb, P. Thaddeus, *Astrophys. J.* **2000**, *530*, 357–361.
[14] D. Fosse, J. Cernicharo, M. Gerin, P. Cox, *Astrophys. J.* **2001**, *552*, 168–174.
[15] P. Thaddeus, M. C. McCarthy, M. J. Travers, C. A. Gottlieb, W. Chen, *Faraday Discuss.* **1998**, *109*, 121–135.
[16] S. J. Blanksby, A. M. McAnoy, S. Dua, J. H. Bowie, *Mon. Not. R. Astron. Soc.* **2001**, *328*, 89–100.
[17] M. C. McCarthy, P. Thaddeus, *J. Mol. Spectrosc.* **2002**, *211*, 235–240.
[18] P. D. Jarowski, F. Diederich, K. N. Houk, *J. Phys. Chem. A* **2006**, *110*, 7237–7246.
[19] P. Botschwina, *Mol. Phys.* **2005**, *103*, 1441–1460.
[20] U. Moelder, P. Burk, I. A. Koppel, *THEOCHEM* **2004**, *712*, 81–89.
[21] I. Y. Ogurtsov, I. Balan, N. N. Gorinchoy, G. Munteanu, *Ann. West Univ. Timisoara Ser. Chem.* **2003**, *12*, 1233–1242.
[22] H. L. Woodcock, H. F. Schaefer, P. R. Schreiner, *J. Phys. Chem. A* **2002**, *106*, 11923–11931.
[23] C. Liang, L. C. Allen, *J. Am. Chem. Soc.* **1991**, *113*, 1873–1878.
[24] J. Kürti, C. Magyar, A. Balázs, P. Rajczy, *Synth. Met.* **1995**, *71*, 1865–1866.
[25] D. Nori-Shargh, F. Deyhimi, J. E. Boggs, S. Jameh-Bozorghi, R. Shakibazadeh, *J. Phys. Org. Chem.* **2007**, *20*, 355–364.
[26] J. P. Kenny, K. M. Krueger, J. C. Rienstra-Kiracofe, H. F. Schaefer III, *J. Phys. Chem. A* **2001**, *105*, 7745–7750.
[27] Y. Zhao, D. G. Truhlar, *J. Phys. Chem. A* **2006**, *110*, 10478–10486.
[28] R. Zahradnik, M. Srnec, Z. Havlas, *Collect. Czech. Chem. Commun.* **2005**, *70*, 559–578.
[29] C. Liang, Y. Xie, H. F. Schaefer, K. S. Kim, H. S. Kim, *J. Am. Chem. Soc.* **1991**, *113*, 2452–2459.
[30] K. B. Wiberg, J. D. Hammer, K. W. Zilm, J. R. Cheeseman, *J. Org. Chem.* **1999**, *64*, 6394–6400.
[31] A. R. Sabirov, J. Bruening, L. A. Chernozatonskii, E. G. Gal'pern, S. V. Lisenkov, I. V. Stankevich, *Fullerenes Nanotubes Carbon Nanostruct.* **2006**, *14*, 489–498.
[32] B. Hong, J. V. Ortega, *Angew. Chem.* **1998**, *110*, 2210–2214; *Angew. Chem. Int. Ed.* **1998**, *37*, 2131–2134.
[33] R. Zahradnik, L. Sroubkova, *Helv. Chim. Acta* **2003**, *86*, 979–1000.
[34] M. Weimer, W. Hieringer, F. D. Sala, A. Görling, *Chem. Phys.* **2005**, *309*, 77–87.
[35] O. Yu. Podkopaeva, Yu. V. Chizhov, *J. Struct. Chem.* **2006**, *47*, 420–426.
[36] A. Markmann, G. A. Worth, L. S. Cederbaum, *J. Chem. Phys.* **2005**, *122*, 144320.
[37] I. Alkorta, J. Elguero, *Struct. Chem.* **2005**, *16*, 77–79.
[38] W. Skibar, H. Kopacka, K. Wurst, C. Salzmann, K.-H. Ongania, F. Fabrizi de Biani, P. Zanello, B. Bildstein, *Organometallics* **2004**, *23*, 1024–1041.
[39] B. Bildstein, O. Loza, Y. Chizhov, *Organometallics* **2004**, *23*, 1825–1835.
[40] G. I. Yranzo, J. Elguero, R. Flammang, C. Wentrup, *Eur. J. Org. Chem.* **2001**, 2209–2220.
[41] N. D. Lang, Ph. Avouris, *Phys. Rev. B* **2000**, *62*, 7325–7329.

[42] G. Koster, W. J. Van der Hart, *Int. J. Mass Spectrom. Ion Process.* **1997**, *163*, 169–175.
[43] S. Olszewski, *Opt. Eng.* **1995**, *334*, 3365–3368.
[44] S. P. Karna, Z. Laskowski, G. B. Talapatra, P. N. Prasad, *J. Phys. Chem.* **1991**, *95*, 6508–6511.
[45] U. Mölder, P. Burk, I. A. Koppel, *THEOCHEM* **2004**, *712*, 81–89.
[46] L. Ravagnan, P. Piseri, M. Bruzzi, S. Miglio, G. Bongiorno, A. Baserga, C. S. Casari, A. Li Bassi, C. Lenardi, Y. Yamaguchi, T. Wakabayashi, C. E. Bottani, P. Milani, *Phys. Rev. Lett.* **2007**, *98*, 216103.
[47] A. Nakamura, P.-J. Kim, N. Hagihara, *J. Organomet. Chem.* **1965**, *3*, 7–15.
[48] A. Nakamura, *Bull. Chem. Soc. Jpn.* **1965**, *38*, 1868–1873.
[49] *Combustion Chemistry: Elementary Reactions to Macroscopic Processes, Faraday Discuss* **2001**, *119*.
[50] M. Frenklach, *Phys. Chem. Chem. Phys.* **2002**, *4*, 2028–2037.
[51] C. E. Baukal, *Oxygen-Enhanced Combustion*, CRS, New York, **1998**.
[52] A. M. Nienow, J. T. Roberts, *Annu. Rev. Phys. Chem.* **2006**, *57*, 105–128.
[53] M. F. Budyka, T. S. Zyubina, A. G. Ryabenko, V. E. Muradyan, S. E. Esipov, N. I. Cherepanova, *Chem. Phys. Lett.* **2002**, *354*, 93–99.
[54] Y.-T. Lin, R. K. Mishra, S.-L. Lee, *J. Phys. Chem. B* **1999**, *103*, 3151–3155.
[55] A. Fernandez-Ramos, J. A. Miller, S. J. Klippenstein, D. G. Truhlar, *Chem. Rev.* **2006**, *106*, 4518–4584.
[56] J. A. Miller, S. J. Klippenstein, *J. Phys. Chem. A* **2006**, *110*, 10528–10544.
[57] N. Hansen, S. J. Klippenstein, J. A. Miller, J. Wang, T. A. Cool, M. E. Law, P. R. Westmoreland, T. Kasper, K. Kohse-Hoeinghaus, *J. Phys. Chem. A* **2006**, *110*, 4376–4388.
[58] N. Hansen, S. J. Klippenstein, C. A. Taatjes, J. A. Miller, J. Wang, T. A. Cool, B. Yang, R. Yang, L. Wei, C. Huang, W. Wang, F. Qi, M. E. Law, P. R. Westmoreland, *J. Phys. Chem. A* **2006**, *110*, 3670–3678.
[59] D. B. Atkinson, J. W. Hudgens, *J. Phys. Chem. A* **1999**, *103*, 4242–4252.
[60] D. K. Hahn, S. J. Klippenstein, J. A. Miller, *Faraday Discuss.* **2001**, *119*, 79–100.
[61] G. B. Bacskay, J. C. Mackie, *Phys. Chem. Chem. Phys.* **2001**, *3*, 2467–2473.
[62] M. Balthasar, M. Frenklach, *Combust. Flame* **2005**, *140*, 130–145.
[63] R. I. Kaiser, *Chem. Rev.* **2002**, *102*, 1309–1358.
[64] Y. Sakakibara, *Bull. Chem. Soc. Jpn.* **1964**, *37*, 1262–1268.
[65] Y. Sakakibara, *Bull. Chem. Soc. Jpn.* **1964**, *37*, 1268–1276.
[66] S. S. Levush, S. S. Abadzhev, V. U. Shvechuk, *Neftekhimiya* **1969**, *9*, 215–220.
[67] K. Liu, *J. Chem. Phys.* **2006**, *125*, 132307.
[68] Y. T. Lee in *Atomic and Molecular Beam Methods* (Ed.: G. Scoles), Oxford University Press, Oxford, **1988**.
[69] P. Casavecchia, G. Capozza, E. Segoloni, *Adv. Ser. Phys. Chem.* **2004**, *14*, 329–381.
[70] R. I. Kaiser, N. Balucani, *Acc. Chem. Res.* **2001**, *34*, 699–706.
[71] M. J. Nam, S. E. Youn, J. H. Choi, *J. Chem. Phys.* **2006**, *124*, 104307.
[72] M. F. Witinski, M. Ortiz-Suarez, H. F. Davis, *J. Chem. Phys.* **2006**, *124*, 094307.
[73] P. L. Houston, *J. Phys. Chem.* **1996**, *100*, 12757–12770.
[74] M. Ahmed, D. S. Peterka, A. G. Suits, *Chem. Phys. Lett.* **1999**, *301*, 372–378.
[75] X. H. Liu, R. L. Gross, A. G. Suits, *J. Chem. Phys.* **2002**, *116*, 5341–5344.
[76] D. Townsend, W. Li, S. K. Lee, R. L. Gross, A. G. Suits, *J. Phys. Chem. A* **2005**, *109*, 8661–8674.
[77] W. Li, C. Huang, M. Patel, D. Wilson, A. G. Suits, *J. Chem. Phys.* **2006**, *124*, 011102.
[78] R. I. Kaiser, A. M. Mebel, *Int. Rev. Phys. Chem.* **2002**, *21*, 307–356.
[79] R. I. Kaiser, C. Ochsenfeld, D. Stranges, M. Head-Gordon, Y. T. Lee, *Faraday Discuss.* **1998**, *109*, 183–204.
[80] Y. Guo, X. Gu, F. Zhang, A. M. Mebel, R. I. Kaiser, *Phys. Chem. Chem. Phys.* **2007**, *9*, 1972–1979.
[81] J. Collin, F. P. Lossing, *J. Am. Chem. Soc.* **1957**, *79*, 5848–5853.
[82] A. Lifshitz, M. Frenklach, A. Burcat, *J. Phys. Chem.* **1975**, *79*, 1148–1152.
[83] A. Lifshitz, M. Frenklach, A. Burcat, *J. Phys. Chem.* **1976**, *80*, 2437–2443.
[84] J. N. Bradley, K. O. West, *J. Chem. Soc. Faraday Trans. 1* **1975**, 967–971.
[85] J. M. Simmie, D. Melvin, *J. Chem. Soc. Faraday Trans. 1* **1978**, 1337–1338.
[86] T. Kakumoto, T. Ushirogouchi, K. Saito, A. Isamaura, *J. Phys. Chem.* **1987**, *91*, 183–189.
[87] C. H. Wu, R. D. Kern, *J. Phys. Chem.* **1987**, *91*, 6291–6296.
[88] Y. Hidaka, T. Chimori, M. Suga, *Chem. Phys. Lett.* **1985**, *119*, 435–437.
[89] Y. Hidaka, T. Nakamura, A. Miyauchi, T. Shirashi, H. Kawano, *Int. J. Chem. Kinet.* **1989**, *21*, 643–666.
[90] J. H. Kiefer, P. S. Mudipalli, S. S. Sidhu, R. D. Kern, B. S. Jursic, K. Xie, H. Chen, *J. Phys. Chem. A* **1997**, *101*, 4057–4071.
[91] C. W. Bauschlicher, S. R. Langhoff, *Chem. Phys. Lett.* **1992**, *193*, 380–385.
[92] M. Frenklach, S. Taki, M. B. Durgaprasad, R. A. Matula, *Combust. Flame* **1983**, *54*, 81–101.
[93] J. A. Miller, S. J. Klippenstein, *J. Phys. Chem. A* **2003**, *107*, 2680–2692.
[94] a) D. A. Ramsay, P. Thistlethwaite, *Can. J. Phys.* **1966**, *44*, 1381–1386; b) W. J. Leigh, *Chem. Rev.* **1993**, *93*, 487–505; c) K. Yamamoto, *Kenkyu Kiyo–Konan Joshi Daigaku* **1990**, *27*, 67–97; d) T. Shimizu in *Photochemistry of Allenes, CRC Handbook of Organic Photochemistry and Photobiology,* CRC, Boca Raton, **2004**, pp. 24/1–24/13; e) R. P. Johnson, *Org. Photochem.* **1985**, *7*, 75–147.
[95] S. Satyapal, R. Bersohn, *J. Phys. Chem.* **1991**, *95*, 8004–8006.
[96] K. Seki, H. Okabe, *J. Phys. Chem.* **1992**, *96*, 3345–3349.
[97] W. M. Jackson, D. S. Anex, R. E. Continetti, B. A. Balko, Y. T. Lee, *J. Chem. Phys.* **1991**, *95*, 7327–7336.
[98] K. Tanaka, T. Harada, K. Sakaguchi, K. Harada, T. Tanaka, *J. Chem. Phys.* **1995**, *103*, 6450–6458.
[99] X. Y. Song, Y. H. Bao, R. S. Urdahl, J. N. Gosine, W. M. Jackson, *Chem. Phys. Lett.* **1994**, *217*, 216–221.
[100] M. L. Lesiecki, K. W. Hicks, A. Orenstein, W. A. Guillory, *Chem. Phys. Lett.* **1980**, *71*, 72–76.
[101] C. K. Ni, J. D. Huang, Y. T. Chen, A. H. Kung, W. M. Jackson, *J. Chem. Phys.* **1999**, *110*, 3320–3325.
[102] J. L. Chang, G. C. Tseng, C. K. Ni, J. D. Huang, Y. T. Chen, *J. Phys. Chem. A* **1999**, *103*, 6063–6073.
[103] W. Z. Sun, K. Yokoyama, J. C. Robinson, A. G. Suits, D. M. Neumark, *J. Chem. Phys.* **1999**, *110*, 4363–4368.
[104] J. D. DeSain, C. A. Taatjes, *J. Phys. Chem. A* **2003**, *107*, 4843–4850.
[105] A. Fahr, A. H. Laufer, *J. Phys. Chem. A* **2005**, *109*, 2534–2539.
[106] H.-Y. Lee, V. V. Kislov, S. H. Lin, A. M. Mebel, D. M. Neumark, *Chem. Eur. J.* **2003**, *9*, 726–740.
[107] J. C. Robinson, N. E. Sveum, S. J. Goncher, D. M. Neumark, *Mol. Phys.* **2005**, *103*, 1765–1783.
[108] S. Harich, Y. T. Lee, X. Yang, *Phys. Chem. Chem. Phys.* **2000**, *2*, 1187–1191.
[109] S. Harich, J. J. Lin, Y. T. Lee, X. Yang, *J. Chem. Phys.* **2000**, *112*, 6656–6665.
[110] R. H. Qadiri, E. J. Feltham, E. E. H. Cottrill, N. Taniguchi, M. N. R. Ashfold, *J. Chem. Phys.* **2002**, *116*, 906–912.
[111] R. H. Qadiri, E. J. Feltham, N. H. Nahler, R. P. Garcia, M. N. R. Ashfold, *J. Chem. Phys.* **2003**, *119*, 12842–12851.
[112] S. Hayakawa, H. Endoh, K. Arakawa, N. Morishita, *Int. J. Mass Spectrom. Ion Processes* **1997**, *171*, 209–214.
[113] K. Alnama, S. Boye-Peronne, S. Douin, F. Innocenti, J. O'Reilly, A. L. Roche, N. Shafizadeh, L. Zuin, D. Gauyacq, *J. Chem. Phys.* **2007**, *126*, 044304.
[114] N. Honjou, J. Pacansky, M. Yoshimine, *J. Am. Chem. Soc.* **1985**, *107*, 5332–5341.
[115] M. Yoshimine, J. Pacansky, N. Honjou, *J. Am. Chem. Soc.* **1989**, *111*, 4198–4209.
[116] M. Yoshimine, J. Pacansky, N. Honjou, *J. Am. Chem. Soc.* **1989**, *111*, 2785–2798.
[117] R. Walsh, *J. Chem. Soc. Faraday Trans. 1* **1976**, 2137–2138.
[118] H. Hopf, H. Priebe, R. Walsh, *J. Am. Chem. Soc.* **1980**, *102*, 1210–1212.
[119] I. M. Bailey, R. Walsh, *J. Chem. Soc. Faraday Trans. 1* **1978**, 1146–1158.
[120] S. P. Walch, *J. Chem. Phys.* **1995**, *103*, 7064–7071.
[121] S. G. Davis, C. K. Law, H. Wang, *J. Phys. Chem. A* **1999**, *103*, 5889–5899.
[122] W. M. Jackson, A. M. Mebel, S. H. Lin, Y. T. Lee, *J. Phys. Chem. A* **1997**, *101*, 6638–6646.
[123] A. M. Mebel, W. M. Jackson, A. H. H. Chang, S. H. Lin, *J. Am. Chem. Soc.* **1998**, *120*, 5751–5763.
[124] T. L. Nguyen, A. M. Mebel, R. I. Kaiser, *J. Phys. Chem. A* **2001**, *105*, 3284–3299.
[125] M. Peric, S. D. Peyerimhoff, R. Buenker, *Mol. Phys.* **1987**, *62*, 1339–1356.
[126] Q. Cui, K. Morokuma, J. F. Stanton, *Chem. Phys. Lett.* **1996**, *263*, 46–53.
[127] R. I. Kaiser, Y. T. Lee, A. G. Suits, *J. Chem. Phys.* **1996**, *105*, 8705–8720.

[128] T. N. Le, H. Y. Lee, A. M. Mebel, R. I. Kaiser, *J. Phys. Chem. A* **2001**, *105*, 1847–1856.
[129] D. Chastaing, P. L. James, I. R. Sims, I. W. M. Smith, *Phys. Chem. Chem. Phys.* **1999**, *1*, 2247–2256.
[130] W. D. Geppert, C. Naulin, M. Costes, G. Capozza, L. Cartechini, P. Casavecchia, G. G. Volpi, *J. Chem. Phys.* **2003**, *119*, 10607–10617.
[131] R. I. Kaiser, T. L. Nguyen, A. M. Mebel, Y. T. Lee, *J. Chem. Phys.* **2002**, *116*, 1318–1324.
[132] R. Wrobel, W. Sander, D. Cremer, E. Kraka, *J. Phys. Chem. A* **2000**, *104*, 3819–3825.
[133] J.-P. Aycard, A. Allouche, M. Cossu, M. Hillerbrand, *J. Phys. Chem. A* **1999**, *103*, 9013–9021.
[134] A. M. Mebel, V. V. Kislov, R. I. Kaiser, *J. Chem. Phys.* **2006**, *125*, 133113.
[135] R. I. Kaiser, A. M. Mebel, A. H. H. Chang, S. H. Lin, Y. T. Lee, *J. Chem. Phys.* **1999**, *110*, 10330–10344.
[136] A. M. Mebel, R. I. Kaiser, Y. T. Lee, *J. Am. Chem. Soc.* **2000**, *122*, 1776–1788.
[137] X. Gu, Y. Guo, F. Zhang, A. M. Mebel, R. I. Kaiser, *Faraday Discuss.* **2006**, *133*, 245–275.
[138] X. Gu, Y. Guo, F. Zhang, A. M. Mebel, R. I. Kaiser, *Chem. Phys.* **2007**, *335*, 95–108.
[139] A. Canosa, A. Paramo, S. D. Le Picard, I. R. Sims, *Icarus* **2007**, *187*, 558–568.
[140] Y. Guo, X. Gu, F. Zhang, A. M. Mebel, R. I. Kaiser, *J. Phys. Chem. A* **2006**, *110*, 10699–10707.
[141] A. M. Mebel, V. V. Kislov, R. I. Kaiser, *J. Phys. Chem. A* **2006**, *110*, 2421–2433.
[142] X. Gu, Y. Guo, A. M. Mebel, R. I. Kaiser, *Chem. Phys. Lett.* **2007**, *449*, 44–52.
[143] R. I. Kaiser, T. L. Lee, T. L. Nguyen, A. M. Mebel, N. Balucani, Y. T. Lee, F. Stahl, P. v. R. Schleyer, H. F. Schaefer III, *Faraday Discuss.* **2001**, *119*, 51–66.
[144] a) N. Krause, A. Hashmi, K. Stephen, *Modern Allene Chemistry, Vol. I and II*, Wiley-VCH, Weinheim, **2004**; b) H. Hopf, *Classics in Hydrocarbon Chemistry: Syntheses, Concepts, Perspectives*, Wiley-VCH, Weinheim, **2000**, p. 558; c) R. Walsh, *Chem. Soc. Rev.* **2005**, *34*, 714–732.
[145] R. I. Kaiser, L. Belau, S. R. Leone, M. Ahmed, Y. Wang, B. J. Braams, J. M. Bowman, *ChemPhysChem* **2007**, *8*, 1236–1239.
[146] Experimental value from J. B. Pedley, *Thermodynamic Data and Structures of Organic Compounds, Vol. 1*, Thermodynamic Research Center, College Station, **1994**.
[147] Recommended theoretical value from S. E. Wheeler, K. A. Robertson, W. D. Allen, H. F. Schaefer III, Y. J. Bomble, J. F. Stanton, *J. Phys. Chem. A* **2007**, *111*, 3819–3830.
[148] Experimental values from *Gas-Phase Ion and Neutral Thermochemistry*: S. G. Lias, J. E. Bartness, J. F. Liebman, J. L. Holmes, R. D. Levin, G. W. Mallard, *J. Phys. Chem. Ref. Data Suppl.* **1988**, *17*. Values in parentheses are less reliable than the other data.
[149] Theoretical values from our present G2M(RCC, MP2) calculations.
[150] Experimental value from W. R. Roth, H. Hopf, C. Horn, *Chem. Ber.* **1994**, *127*, 1781–1795.
[151] Recommended theoretical value from S. E. Wheeler, W. D. Allen, H. F. Schaefer III, *J. Chem. Phys.* **2004**, *121*, 8800–8813.
[152] Theoretical value from G2M(RCC, MP2) calculations. A. M. Mebel, S. H. Lin, X. M. Yang, Y. T. Lee, *J. Phys. Chem. A* **1997**, *101*, 6781–6789.

Received: September 12, 2007
Revised: November 9, 2007

